

Evidence for Higgs boson decays to a low-mass dilepton system and a photon in pp collisions at $\sqrt{s} = 13$ TeV with the ATLAS detector

ATLAS Collaboration

DOI:

[10.1016/j.physletb.2021.136412](https://doi.org/10.1016/j.physletb.2021.136412)

License:

Creative Commons: Attribution (CC BY)

Document Version

Publisher's PDF, also known as Version of record

Citation for published version (Harvard):

ATLAS Collaboration 2021, 'Evidence for Higgs boson decays to a low-mass dilepton system and a photon in pp collisions at $\sqrt{s} = 13$ TeV with the ATLAS detector', *Phys. Lett. B*, vol. 819, 136412.
<https://doi.org/10.1016/j.physletb.2021.136412>

[Link to publication on Research at Birmingham portal](#)

General rights

Unless a licence is specified above, all rights (including copyright and moral rights) in this document are retained by the authors and/or the copyright holders. The express permission of the copyright holder must be obtained for any use of this material other than for purposes permitted by law.

- Users may freely distribute the URL that is used to identify this publication.
- Users may download and/or print one copy of the publication from the University of Birmingham research portal for the purpose of private study or non-commercial research.
- User may use extracts from the document in line with the concept of 'fair dealing' under the Copyright, Designs and Patents Act 1988 (?)
- Users may not further distribute the material nor use it for the purposes of commercial gain.

Where a licence is displayed above, please note the terms and conditions of the licence govern your use of this document.

When citing, please reference the published version.

Take down policy

While the University of Birmingham exercises care and attention in making items available there are rare occasions when an item has been uploaded in error or has been deemed to be commercially or otherwise sensitive.

If you believe that this is the case for this document, please contact UBIRA@lists.bham.ac.uk providing details and we will remove access to the work immediately and investigate.



Evidence for Higgs boson decays to a low-mass dilepton system and a photon in pp collisions at $\sqrt{s} = 13$ TeV with the ATLAS detector

The ATLAS Collaboration*



ARTICLE INFO

Article history:

Received 19 March 2021

Received in revised form 11 May 2021

Accepted 25 May 2021

Available online 31 May 2021

Editor: M. Doser

ABSTRACT

A search for the Higgs boson decaying into a photon and a pair of electrons or muons with an invariant mass $m_{\ell\ell} < 30$ GeV is presented. The analysis is performed using 139 fb^{-1} of proton–proton collision data, produced by the LHC at a centre-of-mass energy of 13 TeV and collected by the ATLAS experiment. Evidence for the $H \rightarrow \ell\ell\gamma$ process is found with a significance of 3.2 over the background-only hypothesis, compared to an expected significance of 2.1 for the Standard Model prediction. The best-fit value of the signal-strength parameter, defined as the ratio of the observed signal yield to the one expected in the Standard Model, is $\mu = 1.5 \pm 0.5$. The Higgs boson production cross-section times the $H \rightarrow \ell\ell\gamma$ branching ratio for $m_{\ell\ell} < 30$ GeV is determined to be $8.7_{-2.7}^{+2.8} \text{ fb}$.

© 2021 The Author. Published by Elsevier B.V. This is an open access article under the CC BY license (<http://creativecommons.org/licenses/by/4.0/>). Funded by SCOAP³.

1. Introduction

In July 2012, the ATLAS and CMS Collaborations at the CERN Large Hadron Collider (LHC) announced the discovery of a new particle with a mass of approximately 125 GeV [1,2]. The observed properties of the particle, such as its couplings to Standard Model (SM) elementary particles, its spin and its parity, are so far consistent with the predictions for the SM Higgs boson [3–7].

Measurements of rare decays of the Higgs boson, such as $H \rightarrow \ell\ell\gamma$ where ℓ is an electron or muon, can probe coupling modifications introduced by possible extensions to the SM [8]. In addition, such three-body Higgs boson decays can be used to probe CP -violation in the Higgs sector [9,10].

Multiple processes contribute to the $H \rightarrow \ell\ell\gamma$ decay: Dalitz decays involving a Z boson or a virtual photon (γ^*) (Fig. 1(a–c)), as well as the decay of the Higgs boson to two leptons and a photon from final-state radiation (FSR) (Fig. 1(d)). Their respective fractions depend on the invariant mass of the dilepton pair, $m_{\ell\ell}$. In this analysis only low-mass dilepton pairs with $m_{\ell\ell} < 30$ GeV are considered. This region is completely dominated by the decay through γ^* [8,11,12]. The contributions of the other processes and interferences are negligible.

Based on a data sample of proton–proton (pp) collisions at $\sqrt{s} = 13$ TeV with an integrated luminosity of 35.9 fb^{-1} , the CMS Collaboration reported a 95% CL upper limit on the production cross-section times branching ratio for the low- $m_{\mu\mu}$ $H \rightarrow \mu\mu\gamma$ process of 4.0 times the SM prediction [13]. In addition, both the ATLAS and CMS Collaborations carried out searches at

$\sqrt{s} = 13$ TeV for the closely related $H \rightarrow Z\gamma$ process [13,14]. The CMS Collaboration also searched for the low- $m_{\ell\ell}$ $H \rightarrow \ell\ell\gamma$ process in the dimuon and dielectron channels in pp collisions at $\sqrt{s} = 8$ TeV [15].

This paper describes a search for $H \rightarrow ee\gamma$ and $H \rightarrow \mu\mu\gamma$ decays with $m_{\ell\ell} < 30$ GeV. When the invariant mass of the two electrons is low and the transverse momentum of the dielectron system is high, their electromagnetic showers can overlap in the calorimeter. Therefore, the search for $ee\gamma$ final states requires the development of dedicated electron trigger and identification algorithms.

The search uses pp collision data at $\sqrt{s} = 13$ TeV recorded with the ATLAS detector during Run 2 of the LHC between 2015 and 2018, corresponding to a total integrated luminosity of 139 fb^{-1} . The sensitivity of the search is enhanced by dividing the selected events into mutually exclusive categories, according to the event topology and lepton flavour. The dominant background is the irreducible non-resonant production of $\ell\ell\gamma$. After event categorisation, the signal yield is extracted by a simultaneous fit of parametric functions to the reconstructed $\ell\ell\gamma$ invariant mass ($m_{\ell\ell\gamma}$) distributions in all categories.

2. ATLAS detector

The ATLAS detector [16] covers nearly the entire solid angle around the collision point.¹ It consists of an inner tracking de-

¹ The ATLAS experiment uses a right-handed coordinate system with its origin at the nominal interaction point (IP) in the centre of the detector and the z -axis along the beam pipe. The x -axis points from the IP to the centre of the LHC ring, and the y -axis points upward. Cylindrical coordinates (r, ϕ) are used in the transverse

* E-mail address: atlas.publications@cern.ch.

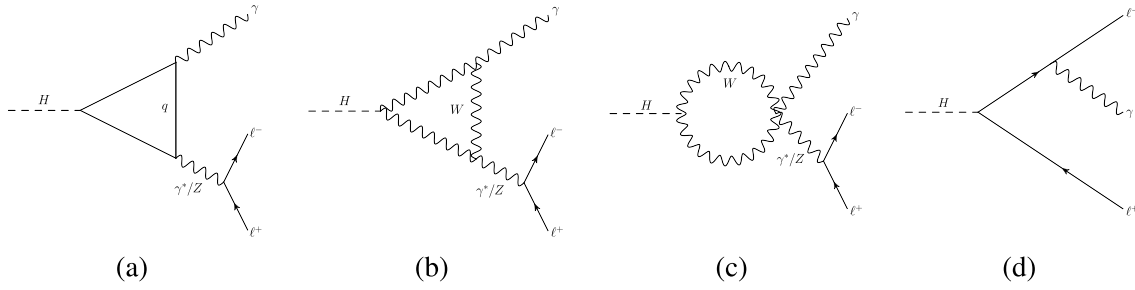


Fig. 1. Representative Feynman diagrams of the $H \rightarrow \ell\ell\gamma$ process.

tor (ID) surrounded by a thin superconducting solenoid providing a 2 T axial magnetic field, electromagnetic (EM) and hadron calorimeters, and a muon spectrometer (MS). The ID covers the pseudorapidity range $|\eta| < 2.5$. It consists of silicon pixel, silicon microstrip, and transition radiation tracking detectors. The silicon pixel detector provides up to four measurements per track. The insertable B-layer (IBL) [17,18] constitutes the innermost layer at a radius of 33.3 mm. It surrounds the beam pipe, which has an inner radius of 23.5 mm. Lead/liquid-argon (LAr) sampling calorimeters provide EM energy measurements with high granularity. A steel/scintillator-tile hadron calorimeter covers the central pseudorapidity range ($|\eta| < 1.7$). The endcap and forward regions are instrumented with LAr calorimeters for both the EM and hadronic energy measurements up to $|\eta| = 4.9$. For $|\eta| < 2.5$, the EM calorimeter is divided into three longitudinal layers, which are finely segmented in η and ϕ , particularly in the first layer. This segmentation allows the measurement of the lateral and longitudinal shower profile, and the calculation of shower shapes [19] used for particle identification and background rejection. The longitudinal segmentation of the EM calorimeter is also exploited to calibrate the energy response of electron and photon candidates [19]. The MS comprises separate trigger and high-precision tracking chambers measuring the deflection of muons in a magnetic field generated by superconducting air-core toroids. The precision chamber system covers the region $|\eta| < 2.7$ with three layers of monitored drift tubes, complemented by cathode-strip chambers in the forward region, where the background is highest. The muon trigger system covers the range $|\eta| < 2.4$ with resistive-plate chambers in the barrel, and thin-gap chambers in the endcap regions.

A two-level trigger system [20] was used during the $\sqrt{s} = 13$ TeV data-taking period. The first-level trigger (L1) is implemented in hardware and uses a subset of the detector information. This is followed by a software-based high-level trigger which runs algorithms similar to those in the offline reconstruction software, reducing the event rate to approximately 1 kHz from the maximum L1 rate of 100 kHz.

3. Data and simulated event samples

The analysed pp collision data correspond to the full recorded LHC Run-2 data set at $\sqrt{s} = 13$ TeV with an integrated luminosity of 139 fb^{-1} after data quality requirements [21]. The events were collected with a combination of single-lepton, dilepton, diphoton, and lepton+photon triggers. Standard electron triggers, which require narrow, isolated EM energy clusters, are efficient if the two electrons in the event have a very small angular separation ΔR_{ee} ,

plane. The polar angle (θ) is measured from the positive z -axis and the azimuthal angle (ϕ) is measured from the positive x -axis in the transverse plane. The pseudorapidity is defined as $\eta = -\ln \tan(\theta/2)$. Angular distance is measured in units of $\Delta R = \sqrt{(\Delta\eta)^2 + (\Delta\phi)^2}$.

as the two electrons produce a cluster that is similar to that of a single electron. For $\Delta R_{ee} > 0.1$, two separate EM clusters are typically produced. For the 2017 and 2018 data-taking periods, a dedicated trigger was introduced which requires at least one photon with $p_T > 35$ GeV and at least one EM cluster with $p_T > 25$ GeV matched to at least one ID track. The EM cluster must have low hadronic leakage, but no requirement is imposed on the width of the shower, which allows this new trigger to recover a significant fraction of the signal with $0.025 < \Delta R_{ee} < 0.1$. More details are provided in Ref. [22]. The overall trigger efficiencies for the $H \rightarrow ee\gamma$ and $H \rightarrow \mu\mu\gamma$ processes are 98% and 96%, respectively (97% combined), relative to the event selection discussed in Section 5. The uncertainty in the trigger efficiency is negligible.

Samples of simulated Monte Carlo (MC) events are crucial for the optimisation of the search strategy and the modelling of the signal and background processes. Simulated $H \rightarrow \gamma^* \gamma \rightarrow \ell\ell\gamma$ signal and $H \rightarrow \gamma\gamma$ background events are used to parameterise these processes, and simulated non-Higgs $\ell\ell\gamma$ events are used to choose analytic functional forms to describe the non-resonant background. The generated MC events, unless stated otherwise, were processed with the full ATLAS detector simulation [23] based on GEANT4 [24]. The effect of multiple pp interactions in the same and neighbouring bunch crossings (pile-up) was included by overlaying minimum-bias events simulated with PYTHIA 8.186 [25] using the NNPDF2.3LO parton distribution function (PDF) set [26] and the A3 set [27] of tuned parameters. The MC events were weighted to reproduce the distribution of the number of interactions per bunch crossing observed in the data.

Higgs boson production in the gluon-gluon fusion (ggF) and vector-boson fusion (VBF) production modes, as well as in quark-initiated associated production with a W or Z boson ($q\bar{q}/qg \rightarrow VH$) or with two top quarks ($t\bar{t}H$) was modelled with the POWHEG-Box v2 MC event generator [28–32]. POWHEG-Box v2 was interfaced with PYTHIA 8 [25] to simulate the $H \rightarrow \gamma^* \gamma \rightarrow \ell\ell\gamma$ and $H \rightarrow \gamma\gamma$ decays. PYTHIA also provides parton showering, hadronisation and the underlying event. The PDF4LHC15 PDF set [33] was used, except for $t\bar{t}H$, where the NNPDF3.0nlo PDF set [26] was used. For the ggF process, the POWHEG NNLOPS program [34,35] achieves next-to-next-to-leading-order (NNLO) accuracy in QCD for inclusive observables after reweighting the Higgs boson rapidity spectrum [36]. The simulation reaches next-to-leading-order (NLO) accuracy in QCD for the VBF, VH , and $t\bar{t}H$ processes. For VH , the MiNLO technique [37–39] was applied. No simulated samples are available for gluon-initiated associated production with a Z boson ($gg \rightarrow ZH$) and associated production with two b -quarks (bbH). Their minor contribution, 1% of the expected Higgs boson production, is modelled using the acceptances from the $q\bar{q}/qg \rightarrow ZH$ and ggF samples, respectively.

Alternative $H \rightarrow \gamma\gamma$ samples are considered for the ggF and VBF processes, where HERWIG 7 [40] was used instead of PYTHIA 8 to provide parton showering. Weights were calculated by comparing the generator-level Higgs boson transverse momentum and jet distributions in these samples with the distributions obtained from

the nominal $H \rightarrow \gamma\gamma$ samples. The weights are applied to the $H \rightarrow \gamma^*\gamma \rightarrow \ell\ell\gamma$ ggF and VBF samples to estimate the effect of varying the parton shower and underlying event.

The mass of the Higgs boson was set in the simulation to $m_H = 125$ GeV and its width to $\Gamma_H = 4.1$ MeV [41]. The Higgs mass peak position in the simulation was corrected to account for the small difference relative to the measured value of 125.09 GeV [42] (see Section 6); otherwise the effect on the kinematics is neglected.

The signal and $H \rightarrow \gamma\gamma$ samples were normalised with the best available theoretical calculations of the corresponding SM production cross-sections at $m_H = 125.09$ GeV, which are available at next-to-next-to-next-to-leading order (N³LO) in QCD with NLO electroweak (EW) corrections for ggF [41,43–54], at approximate-NNLO in QCD with NLO EW corrections for VBF [41,55–57], at NNLO in QCD with NLO EW corrections for $q\bar{q}/qg \rightarrow VH$ [41,58–65] and at NLO in QCD with NLO electroweak corrections for $t\bar{t}H$ [41,66–69]. The accuracy of the calculation is NNLO in QCD for bbH [70–72], and NLO in QCD with next-to-leading-logarithm (NLL) corrections for $gg \rightarrow ZH$ [41,61].

There are multiple calculations of the $H \rightarrow \ell\ell\gamma$ branching ratios for different slices of phase space [8,11,12,73–76]. The $H \rightarrow \ell\ell\gamma$ branching ratios used in this analysis are $\mathcal{B}(H \rightarrow ee\gamma) = 7.20 \times 10^{-5}$ and $\mathcal{B}(H \rightarrow \mu\mu\gamma) = 3.42 \times 10^{-5}$, as estimated with PYTHIA 8 for $m_{\ell\ell} < 30$ GeV. Their sum corresponds to $\sim 5\%$ of the $H \rightarrow \gamma\gamma$ branching ratio. When extrapolated to a common phase space, the PYTHIA 8 estimate agrees with the predictions of Refs. [74,76] within a relative difference of 3%. Currently, no theoretical uncertainty calculation exists for the low- $m_{\ell\ell}$ $H \rightarrow \ell\ell\gamma$ branching ratio. Therefore, the theoretical uncertainties in the $H \rightarrow \gamma\gamma$ and $H \rightarrow Z\gamma$ branching ratios are considered [12], and the larger of the two uncertainties is used, which corresponds to the 5.8% relative uncertainty in the $H \rightarrow Z\gamma$ branching ratio [41].

The background originates mainly from non-resonant $\ell\ell\gamma$ production. Events were simulated with the SHERPA 2.2.8 [77] generator based on LO matrix elements for $\ell\ell\gamma$ production with up to three additional partons and using the NNPDF3.0 PDF set [78]. The SHERPA simulation includes parton shower, fragmentation and underlying-event modelling. As the statistical uncertainties in the simulated $\ell\ell\gamma$ background samples are a limiting factor when studying the background modelling at the level required by the small signal-to-background ratio, a procedure was developed to generate significantly larger samples. These are based on events generated using the SHERPA 2.2.8 configuration described above with object efficiencies approximated by parameterisations rather than using the full ATLAS detector simulation and reconstruction software. The parameterisations, extracted from fully simulated MC samples, reproduce the reconstruction and selection efficiencies of detector-level objects via event weighting. Comparisons with a sample that underwent the full ATLAS detector simulation, and whose effective luminosity is greater than the data luminosity, show good agreement within the statistical uncertainties.

4. Object selection

Events are required to have a collision vertex associated with at least two tracks with transverse momentum $p_T > 0.5$ GeV each. In the case of multiple vertices, the vertex with the largest $\sum p_T^2$ of the associated tracks is considered to be the primary vertex.

Muon candidates are obtained by matching high-quality tracks in the MS and ID. Standalone MS tracks are used to extend the muon reconstruction beyond the ID acceptance to $2.5 < |\eta| < 2.7$. Muon candidates are required to satisfy the *medium* identification criteria [79,80], be within $|\eta| < 2.7$ and have $p_T > 3$ GeV. Muon candidates with an associated ID track must be matched to the primary vertex by having a longitudinal impact parameter Δz_0 that satisfies $|\Delta z_0 \cdot \sin\theta| < 0.5$ mm, where θ is the polar angle of the

track. The significance of the transverse impact parameter d_0 calculated relative to the measured beam-line position is required to be $|d_0|/\sigma_{d_0} < 3$, where σ_{d_0} is the uncertainty in d_0 . A subset of the muon candidates are also required to be isolated from additional activity in the tracking detector and in the calorimeters, using a loose isolation selection [79,80]. The efficiency of the muon reconstruction and identification, as well as the momentum calibration, including the associated systematic uncertainties, is estimated as described in Refs. [79,80].

Photon and electron candidates are reconstructed from energy clusters in the calorimeters which are formed using an algorithm based on dynamical, topological cell-clustering [19]. Candidates in the transition region between the barrel and endcap EM calorimeters, $1.37 < |\eta| < 1.52$, are excluded. The performance of the electron and photon reconstruction, including the associated systematic uncertainties, is studied in Ref. [19].

Photon candidates can be either unconverted or converted. In the latter case, a track or conversion vertex is matched to the EM cluster. Photon candidates are required to satisfy $p_T > 20$ GeV and $|\eta| < 2.37$, and pass the *tight* identification requirements [19,81] as well as a loose isolation selection [19].

The energy of the EM clusters associated with the photon and electron candidates is corrected in successive steps using a combination of simulation-based and data-driven correction factors [19]. The simulation-based calibration regression is optimised separately for electrons, unconverted photons and converted photons. The resolution of the energy response is corrected in the simulation to match the resolution observed in data using $Z \rightarrow ee$ events, by smearing the electron energy such that the width of the simulated Z boson peak matches the width observed in data.

Because of the event kinematics of the signal process, it is common for the energy deposits of the two electrons in the EM calorimeter to be reconstructed as a single cluster. Therefore, two types of electron candidates are defined, each with its own selection criteria: one in which a topological cluster of energy deposits is associated with one selected ID track (*resolved* electron [82]), representing a single electron, and one in which a topological cluster is associated with two selected ID tracks (*merged* ee), representing a merged electron pair. Each ID track considered must satisfy $|\Delta z_0 \cdot \sin\theta| < 0.5$ mm and $|d_0|/\sigma_{d_0} < 5$. Resolved electron candidates must satisfy the *medium* likelihood-based identification criteria [19,82], have $p_T > 4.5$ GeV and be within $|\eta| < 2.47$. A subset of the resolved electron candidates are also required to pass a loose isolation requirement [19].

ID tracks considered for merged electrons must have opposite charge, $p_T > 5$ GeV, $|\eta| < 2.5$, and at least seven hits in the pixel and microstrip detectors combined. To suppress backgrounds from converted photons, tracks must also have a hit in the innermost pixel layer, and merged-electron candidates are rejected if they match a conversion vertex with a radius larger than 20 mm whose momentum agrees better with the cluster energy than the momentum of the track that geometrically matches the cluster best. Because the kinematic behaviour of merged electrons in the calorimeter most closely resembles a photon converting in the material close to the interaction vertex, the energy of the merged- ee object is calibrated as a converted photon with a conversion radius set to $r_{\text{conv}} = 30$ mm calculated relative to the measured beam-line position. As presented in Fig. 2(a), this treatment is found to induce minimal bias in the dielectron energy measurement. To cover remaining differences between the simulated detector response to converted photons and merged- ee objects, the difference between the squares of the energy resolutions for converted photons and merged- ee objects in the MC simulation is treated as the square of an additional energy resolution uncertainty. The four-momentum of the merged- ee candidate is constructed using the calibrated en-

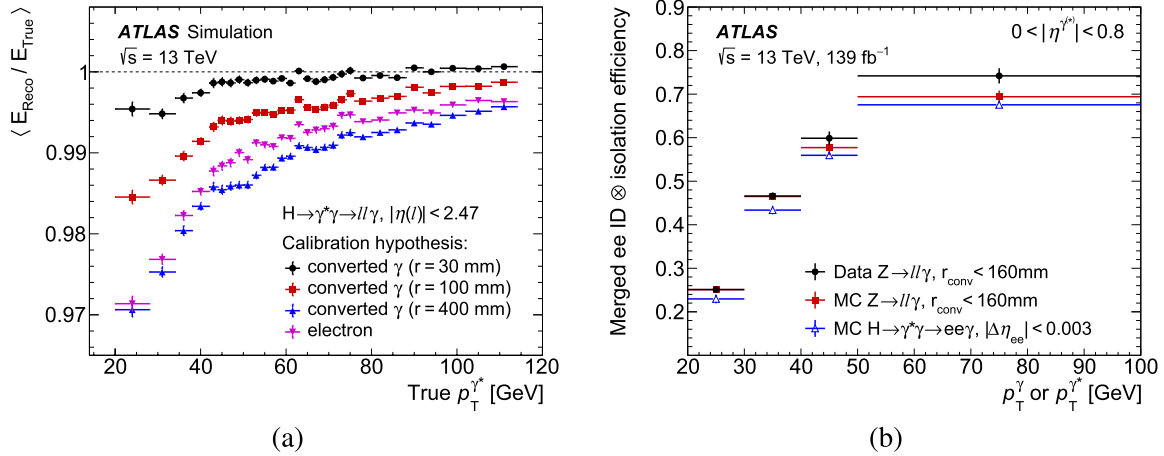


Fig. 2. (a) Ratio of reconstructed to true merged- ee energy in simulated $H \rightarrow \gamma^* \gamma \rightarrow ee \gamma$ events as a function of the true merged- ee p_T for several energy calibration techniques. The merged- ee object is calibrated as a photon with a conversion radius of 30 mm (black circles, analysis choice), 100 mm (red upward triangles) or as an electron (purple downward triangles). (b) Combined merged- ee identification and isolation efficiency extracted from $Z \rightarrow ll \gamma$ events with a photon that converts at a radius of $r_{\text{conv}} < 160$ mm. The efficiencies are shown for photons with $|\eta| < 0.8$ as a function of p_T . Data (black circles) are compared with simulated $Z \rightarrow ll \gamma$ events (red squares). The resulting efficiencies are also compared with efficiencies in simulated $H \rightarrow \gamma^* \gamma \rightarrow ee \gamma$ events (blue triangles). On all points, the vertical error bars indicate the statistical uncertainties.

ergy and the direction and invariant mass obtained from the vertex reconstructed from the two electron-track candidates [83].

Merged- ee candidates are required to have $|\eta| < 2.37$ (excluding $1.37 < |\eta| < 1.52$) and $p_T > 20$ GeV, and satisfy dedicated identification requirements, as the standard electron criteria have a low efficiency for objects with closely spaced energy deposits or broader EM showers. For the merged- ee identification, a multivariate discriminator is trained to separate the $\gamma^* \rightarrow ee$ signal objects from jets or single electrons. The input variables for the training include shower shape variables [82], the information provided by the transition radiation tracker [84], and the kinematic information from the cluster and ID tracks. Merged- ee candidates are also required to pass a tight isolation requirement [19]. A combined efficiency of $\sim 50\%$ for the merged- ee identification and isolation is achieved for $H \rightarrow \gamma^* \gamma \rightarrow ee \gamma$ events. Since photons with a relatively small conversion radius offer a signature similar to that of merged- ee objects, the merged- ee identification and isolation efficiency is measured in data using a tag-and-probe method with FSR photons from Z boson radiative decays ($Z \rightarrow ll \gamma$). Candidate $Z \rightarrow ll \gamma$ events are selected similarly to those in Ref. [81]. Only two-track converted photons with $r_{\text{conv}} < 160$ mm, corresponding to conversions inside the silicon pixel detector volume, are considered. The $Z \rightarrow ll \gamma$ and background yields are estimated from a fit to the $m_{ll \gamma}$ distribution in data. The extracted efficiencies are compared with the efficiencies estimated from simulated $Z \rightarrow ll \gamma$ events as shown in Fig. 2(b) for photons with $|\eta| < 0.8$. The resulting p_T - and η -dependent data/simulation scale factors are between 0.9 and 1.1 and are used to correct the identification and isolation efficiencies of the simulated $H \rightarrow \gamma^* \gamma \rightarrow ee \gamma$ events. The statistical uncertainties of the scale factors are taken into account. In addition, a systematic uncertainty is assessed for the background modelling by varying the selection criteria of the $m_{ll \gamma}$ background template. The total uncertainty reaches 2% for $20 < p_T < 30$ GeV and 9% for $p_T > 50$ GeV. Fig. 2(b) also shows a comparison of the extracted efficiencies with efficiencies in simulated $H \rightarrow \gamma^* \gamma \rightarrow ee \gamma$ events where an additional generator-level requirement of $|\Delta \eta_{ee}| < 0.003$ is used. This requirement is applied in order to better match the signal signature to the converted photon signature in the detector; approximately 70% of the merged- ee objects in the signal sample pass it. The efficiencies of converted photons and the merged- ee objects agree within 10%

for $p_T < 30$ GeV and within 5% for $p_T > 30$ GeV in the entire η range.

Jets are reconstructed from topological clusters [85] using the anti- k_t algorithm [86] with a radius parameter of 0.4 and are required to have $p_T > 20$ GeV and $|\eta| < 4.4$. Jets produced in pile-up interactions are suppressed by requiring that those with $p_T < 60$ GeV and $|\eta| < 2.4$ pass a selection based on a jet vertex tagging algorithm [87].

5. Event selection

Candidate $H \rightarrow \gamma^* \gamma \rightarrow ll \gamma$ events must have at least one reconstructed photon, and at least one opposite-charge, same-flavour pair of leptons (muons or resolved electrons) or one merged- ee object. One of the muons (resolved electrons) in the lepton pair must have $p_T > 11$ (13) GeV, to match the p_T thresholds used in the dilepton triggers. As discussed above, the merged- ee p_T is required to be larger than 20 GeV. If the leading photon overlaps with one of the EM clusters (resolved electrons or merged- ee) forming the γ^* candidate within $\Delta R < 0.02$, the photon is discarded and the next-highest- p_T photon is considered. No isolation requirement is applied to the subleading lepton (muon or resolved electron) as it is within the isolation cone of the leading lepton in the majority of events. Additionally, if the subleading lepton (muon or electron) falls within the isolation cone of the leading lepton, it is not included in the calculation of the isolation variable.

Muon pairs are given the highest priority if there are lepton pairs of different flavours in one event. If no opposite-charge muon pair satisfying the requirements above is found, the electron-pair candidates are considered. The resolved electron pair or merged- ee object with the highest vector-sum of the p_T of the associated ID tracks is selected.

In order to suppress events arising from FSR processes, events are rejected if the photon is within a $\Delta R = 0.4$ cone around either of the selected leptons. If the axis of a jet is within $\Delta R = 0.4$ of the photon or a muon, or within $\Delta R = 0.2$ of an electron (merged or resolved), the jet is discarded. However, if the electron-jet angular separation is $0.2 < \Delta R < 0.4$, the electron and therefore the event is discarded.

To suppress events involving Z boson decays, the dilepton invariant mass must satisfy $m_{\ell\ell} < 30$ GeV. To remove $J/\psi \rightarrow \ell\ell$ production, events with a dimuon (dielectron) invariant mass in

Table 1

Number of data events selected in each analysis category in the $m_{\ell\ell\gamma}$ mass range of 110–160 GeV. In addition, the following numbers are given: number of $H \rightarrow \gamma^*\gamma \rightarrow \ell\ell\gamma$ events in the smallest $m_{\ell\ell\gamma}$ window containing 90% of the expected signal (S_{90}), the non-resonant background in the same interval (B_{90}^N) as estimated from fits to the data sidebands using the background models described in Section 6, the resonant background in the same interval ($B_{H\rightarrow\gamma\gamma}$), the expected signal purity $f_{90} = S_{90}/(S_{90} + B_{90})$, and the expected significance estimate defined as $Z_{90} = \sqrt{2((S_{90} + B_{90}) \ln(1 + S_{90}/B_{90}) - S_{90})}$ where $B_{90} = B_{90}^N + B_{H\rightarrow\gamma\gamma}$. $B_{H\rightarrow\gamma\gamma}$ is only relevant for the electron categories and is marked as “–” otherwise.

Category	Events	S_{90}	B_{90}^N	$B_{H\rightarrow\gamma\gamma}$	f_{90} [%]	Z_{90}
ee resolved VBF-enriched	10	0.4	1.6	0.009	20	0.3
ee merged VBF-enriched	15	0.8	2.0	0.07	27	0.5
$\mu\mu$ VBF-enriched	33	1.3	5.9	–	18	0.5
ee resolved high- $p_{T\ell}$	86	1.1	12	0.02	9	0.3
ee merged high- $p_{T\ell}$	162	2.5	18	0.2	12	0.6
$\mu\mu$ high- $p_{T\ell}$	210	4.0	34	–	11	0.7
ee resolved low- $p_{T\ell}$	3713	22	729	0.5	2.9	0.8
ee merged low- $p_{T\ell}$	5103	29	942	2	3.0	1.0
$\mu\mu$ low- $p_{T\ell}$	9813	61	1750	–	3.4	1.4

the range $2.9 < m_{\mu\mu} < 3.3$ GeV ($2.5 < m_{ee} < 3.5$ GeV) are excluded. Similarly, events with a dimuon (dielectron) invariant mass in the range $9.1 < m_{\mu\mu} < 10.6$ GeV ($8.0 < m_{ee} < 11.0$ GeV) are rejected to avoid $\Upsilon(nS) \rightarrow \ell\ell$ contamination.

The invariant mass of the $\ell\ell\gamma$ system is required to satisfy $110 < m_{\ell\ell\gamma} < 160$ GeV. Additionally, both the photon and dilepton momenta must satisfy $p_T > 0.3 \cdot m_{\ell\ell\gamma}$.

The selected events are classified into mutually exclusive categories, depending on the lepton types and event topologies. The VBF-enriched categories, which have the best expected signal-to-background ratio, but the lowest event count, are defined as follows. Events must contain at least two jets with $p_T > 25$ GeV. If the leading or subleading jet is a forward jet (defined as a jet with $|\eta| > 2.5$), it is required to have $p_T > 30$ GeV to suppress jets originating from pile-up. In addition, the invariant mass of the two leading jets, m_{jj} , must be greater than 500 GeV, and the pseudorapidity separation between the two leading jets, $|\Delta\eta_{jj}|$, greater than 2.7. The quantity $|\eta_{\ell\ell\gamma} - 0.5(\eta_{j1} + \eta_{j2})|$ [88] is required to be less than 2.0, where $\eta_{\ell\ell\gamma}$ is the pseudorapidity of the $\ell\ell\gamma$ system and η_{j1} (η_{j2}) is the pseudorapidity of the leading (subleading) jet. The selected leptons and the photon must be separated from the two jets by $\Delta R > 1.5$. Additionally, the azimuthal separation between the $\ell\ell\gamma$ system and the system formed by the two jets must be greater than 2.8. These jet variables are expected to have a different shape for the VBF signal and the background from QCD processes.

The $p_{T\ell}$ is defined as the component of the transverse momentum of the $\ell\ell\gamma$ system that is perpendicular to the difference of the three-momenta of the dilepton system and the photon candidate ($p_{T\ell} = |\vec{p}_T^{\ell\ell\gamma} \times \hat{t}|$, where $\hat{t} = (\vec{p}_T^{\ell\ell} - \vec{p}_T^\gamma)/|\vec{p}_T^{\ell\ell} - \vec{p}_T^\gamma|$). This quantity is strongly correlated with the transverse momentum of the $\ell\ell\gamma$ system, but has better experimental resolution [89,90]. Events failing the VBF-enriched selection, but having $p_{T\ell} > 100$ GeV, are assigned to the high- $p_{T\ell}$ category, which has a lower expected signal-to-background ratio than the VBF-enriched category, but is expected to have more events. The high- $p_{T\ell}$ category is expected to have an increased fraction of VBF and VH events as these production modes lead on average to higher Higgs boson p_T than ggF production.

The vast majority of selected events do not fall into the VBF-enriched or high- $p_{T\ell}$ categories discussed above, and are placed into the low- $p_{T\ell}$ category. The full list of all categories considered in the analysis, together with the expected yields for a 125.09 GeV Higgs boson decaying into $\ell\ell\gamma$, is shown in Table 1. The table also summarises the observed number of events in data in the $m_{\ell\ell\gamma}$ mass range of 110–160 GeV.

6. Signal and background modelling

To extract the observed signal yield, parametric functions are chosen to model the $\ell\ell\gamma$ invariant mass distributions of signal and background in each analysis category. A combined model is built from these functions and fit to the selected data in the $m_{\ell\ell\gamma}$ range of 110–160 GeV, simultaneously in all categories.

The signal model, including its parameters, is obtained by fitting a double-sided Crystal Ball function (DSCB) [91,92] to the $m_{\ell\ell\gamma}$ distribution obtained from the $H \rightarrow \gamma^*\gamma \rightarrow \ell\ell\gamma$ samples described in Section 3 after applying the event selection and categorisation from Section 5. The DSCB function features a Gaussian core and asymmetric power-law tails. A shift of +0.09 GeV is applied to the mean of the Gaussian function to account for the fact that the sample assumes a Higgs boson mass of 125 GeV. The effective signal mass resolution, defined as half the width containing 68% of the signal events, depends on the category and lies between 1.6 GeV (ee -merged high- $p_{T\ell}$ category) and 2.2 GeV (ee -resolved low- $p_{T\ell}$ category).

The $H \rightarrow \gamma\gamma$ process, which contributes as background to the electron categories through converted photons, is modelled using the same functions and parameters as the signal in the respective categories, and is normalised to the predicted SM yield. The parameterisations are compatible with the statistically limited distributions obtained from simulated $H \rightarrow \gamma\gamma$ events. This background contribution is relatively small (<2.5% and <7% of the expected $H \rightarrow \gamma^*\gamma \rightarrow \ell\ell\gamma$ signal in the ee -resolved channel and ee -merged channel, respectively) and is taken into account in the fitting procedure.

The non-resonant background is also estimated with parametric functions. The background normalisation and function parameters are allowed to float in the fit to data. The chosen functional forms are based on background templates that are built taking into account the contributions of different processes to the background. The function choice is performed separately for each category.

The dominant part of the background originates from the non-resonant $\ell\ell\gamma$ process. There is also a smaller background from events with misidentified photons, electrons, or muons. To estimate the fraction of events with a misidentified photon, a control region is formed using the signal selection, but dropping the photon isolation requirement and using it as a discriminating variable in a template fit. A background template enriched in events with misidentified photons is built by inverting the photon identification selection, with the prompt-photon contamination removed by subtracting its distribution found in simulated events. The template normalisation is obtained in the background-dominated sideband of the photon isolation distribution for each category separately. In the signal region, about 10% of all selected events have a misidentified photon, independently of the category. The fraction of events with a misidentified electron or muon that is in fact a hadronic jet, a lepton from heavy-flavour decays or an electron from a photon conversion, is estimated in a similar manner, using a control region in which the isolation selection is dropped for the softer lepton. The estimated fractions of events with misidentified leptons are 4% in the $\mu\mu$ low- $p_{T\ell}$ category, 2% in the ee -merged low- $p_{T\ell}$ category, and 30% in the ee -resolved low- $p_{T\ell}$ category. Events in the last category are separated into two groups depending on the angular distance between the electrons, as two populations with different misidentified-electron rates and mass distributions were found. The numbers in the other categories are extracted as well, but suffer from fairly large statistical uncertainties.

The invariant mass template for the non-resonant $\ell\ell\gamma$ background is built from the simulated events described in Section 3. The invariant mass templates for events with misidentified ob-

jects are obtained from background-dominated control regions, and scaled by the yields derived above. Reasonable agreement is observed between the templates containing the sum of all backgrounds and the sidebands of the $m_{\ell\ell\gamma}$ distributions in data (105–120 GeV and 130–160 GeV).

The choice of fit function for the non-resonant background is made in each category using signal-plus-background fits to the constructed background-only template by measuring the bias associated with each function, expressed as the number of fitted signal events, and choosing the function with the smallest number of degrees of freedom that satisfies the bias criteria described below.

The functional forms used to model the background are selected from the following: exponential ($e^{\alpha m_{\ell\ell\gamma}}$), exponential of a second-order polynomial ($e^{\alpha m_{\ell\ell\gamma} + \beta m_{\ell\ell\gamma}^2}$), and a power-law function ($m_{\ell\ell\gamma}^\alpha$), where α and β are free parameters. Signal hypotheses with m_H ranging from 121 GeV to 129 GeV are tested in steps of 1 GeV, and the fit bias is evaluated as the absolute maximum bias over this range (referred to as the ‘spurious signal’ in the following), similar to what is done in Ref. [1]. A function passes the test if the spurious signal is less than 10% of the expected number of $H \rightarrow \gamma^*\gamma \rightarrow \ell\ell\gamma$ events or less than 20% of the statistical uncertainty of the fitted spurious signal due to the expected number of background events. To account for statistical fluctuations in the background template, the criteria are relaxed by the statistical uncertainty due to the template [93]. Furthermore, in a background-only fit of the template in the mass range $110 < m_{\ell\ell\gamma} < 160$ GeV, the function must pass a χ^2 test with a probability larger than 1%. As described in Ref. [93], an additional check is performed by fitting both the chosen function and a function belonging to the same family with one more degree of freedom to the sidebands of the $m_{\ell\ell\gamma}$ distribution in data, to ensure the data do not prefer the more complex function. Following the procedure described above, the power-law function is selected for all categories, except for the $\mu\mu$ low- $p_{T\ell}$ and ee -merged low- $p_{T\ell}$ categories, which are best described by the second-order exponential polynomial, and the ee -resolved VBF-enriched category, for which the exponential function is chosen.

An unbinned extended likelihood function is formed from the product of each category’s parameterised signal-plus-background probability density function. Systematic uncertainties are considered in the form of nuisance parameters with Gaussian or log-normal constraints. They are correlated across all categories, except for the spurious-signal uncertainties. The latter are implemented for each category as a signal-like component with a yield parameter that is constrained by a Gaussian function, centred at zero, with a width corresponding to the estimated spurious signal. The Higgs boson mass is set to 125.09 ± 0.24 GeV [42].

The parameter of interest is the signal strength μ , which is defined as the ratio of the measured signal yield to the SM expectation, taking into account the uncertainties on the latter. The corresponding profile likelihood ratio is maximised to extract the best-fit μ [94]. A possible excess over the background-only hypothesis is quantified by a p -value using the profile likelihood ratio, evaluated for a vanishing $H \rightarrow \ell\ell\gamma$ branching ratio, as a test statistic. For all results, the asymptotic approximation is used [94]. Cross-checks of the best-fit μ and the p -value extracted with pseudo-experiments show good agreement with those obtained using the asymptotic approximation.

The measurement of the signal strength can be converted into a measurement of the Higgs boson production cross-section times the $H \rightarrow \ell\ell\gamma$ branching ratio in the fiducial region $m_{\ell\ell} < 30$ GeV. In this case, the included theory uncertainties are adjusted as discussed in Section 7, and the acceptance is extracted with the simulated samples described in Section 3.

7. Systematic uncertainties

The total observed systematic uncertainty in the signal strength measurement is 11%, which is about 35% of the size of the statistical uncertainty. Therefore, systematic uncertainties do not play a dominant role in this analysis.

The dominant experimental systematic uncertainties are due to the estimated biases in the fitted signal events (spurious signal, see Section 6). The corresponding uncertainty in the observed signal strength amounts to 6.1%. Other non-negligible systematic uncertainties relate to photon and lepton identification efficiencies in the simulated signal samples, in particular for merged- ee objects, as well as the energy/momentum calibration (see Section 4). Including jet uncertainties, which have a much smaller impact, these add up to 4.0%.

The uncertainty in the combined 2015–2018 integrated luminosity is 1.7% [95], obtained using the LUCID-2 detector [96] for the primary luminosity measurements. Uncertainties in the pile-up modelling contribute 1.7%. Uncertainties in the estimate of the $H \rightarrow \gamma\gamma$ background have a small impact of 0.7%. They include uncertainties in the photon–electron fake rate, and the uncertainties in the $\sigma(H) \times \mathcal{B}(H \rightarrow \gamma\gamma)$ measurement [93].

The assumed uncertainty in the $H \rightarrow \gamma^*\gamma \rightarrow \ell\ell\gamma$ branching ratio contributes 5.8%. The choice of QCD scales impacts the number and distribution of signal events in the different categories and is evaluated for the ggF, VBF, and VH production modes using a scheme similar to the one discussed in Ref. [93]. The corresponding uncertainty in the measured signal strength is 4.7%. Uncertainties in the PDF are evaluated using the eigenvectors of the PDF4LHC15 PDF set [33] and have a smaller effect of 2.3%. A conservative uncertainty of 50% is assigned to the normalisation of the $t\bar{t}H$, $gg \rightarrow ZH$, and bbH production modes, as no dedicated $H \rightarrow \gamma^*\gamma \rightarrow \ell\ell\gamma$ samples are available, with an impact of 0.8%. Parton shower uncertainties contribute only 0.3%.

For the $\sigma(H) \times \mathcal{B}(H \rightarrow \ell\ell\gamma)$ measurement, the effect of the theory uncertainties is reduced to 1.1% for the QCD scale and 0.9% for the PDF uncertainty, as only acceptance effects are considered, whereas the uncertainties in the predicted cross-sections and branching ratio are not applicable to this measurement.

8. Results

The $m_{\ell\ell\gamma}$ distributions of the selected events and the result of the global fit of the parametric signal-plus-background models to the data are shown in Fig. 3 for each event category.

The best-fit value of the signal-strength parameter is $\mu = 1.5 \pm 0.5 = 1.5 \pm 0.5$ (stat.) $^{+0.2}_{-0.1}$ (syst.), while the corresponding expected SM value is $\mu_{\text{exp}} = 1.0 \pm 0.5 = 1.0 \pm 0.5$ (stat.) $^{+0.2}_{-0.1}$ (syst.). The best-fit signal strength in the muon (electron) channel, obtained from a fit with two separate signal-strength parameters, is $\mu_{\mu\mu} = 1.9 \pm 0.7$ ($\mu_{ee} = 1.0 \pm 0.7$). Fig. 4 shows the results of the fit when the signal strength in each category is allowed to float independently. As anticipated in Table 1, the low- $p_{T\ell}$ categories, especially in the $\mu\mu$ channel, have the smallest uncertainties. It can be seen that all categories yield results that are consistent with each other and with the result of the single- μ fit.

For illustration, Fig. 5 shows the $m_{\ell\ell\gamma}$ distribution, with every data event reweighted by a category-dependent weight $\ln(1 + S_{90}/B_{90})$, where S_{90} is the number of signal events in the smallest window containing 90% of the expected signal and B_{90} is the expected number of background events in the same window, which consists of the resonant $H \rightarrow \gamma\gamma$ background as well as the non-resonant background. The latter is estimated from fits to the data sidebands using the background models.

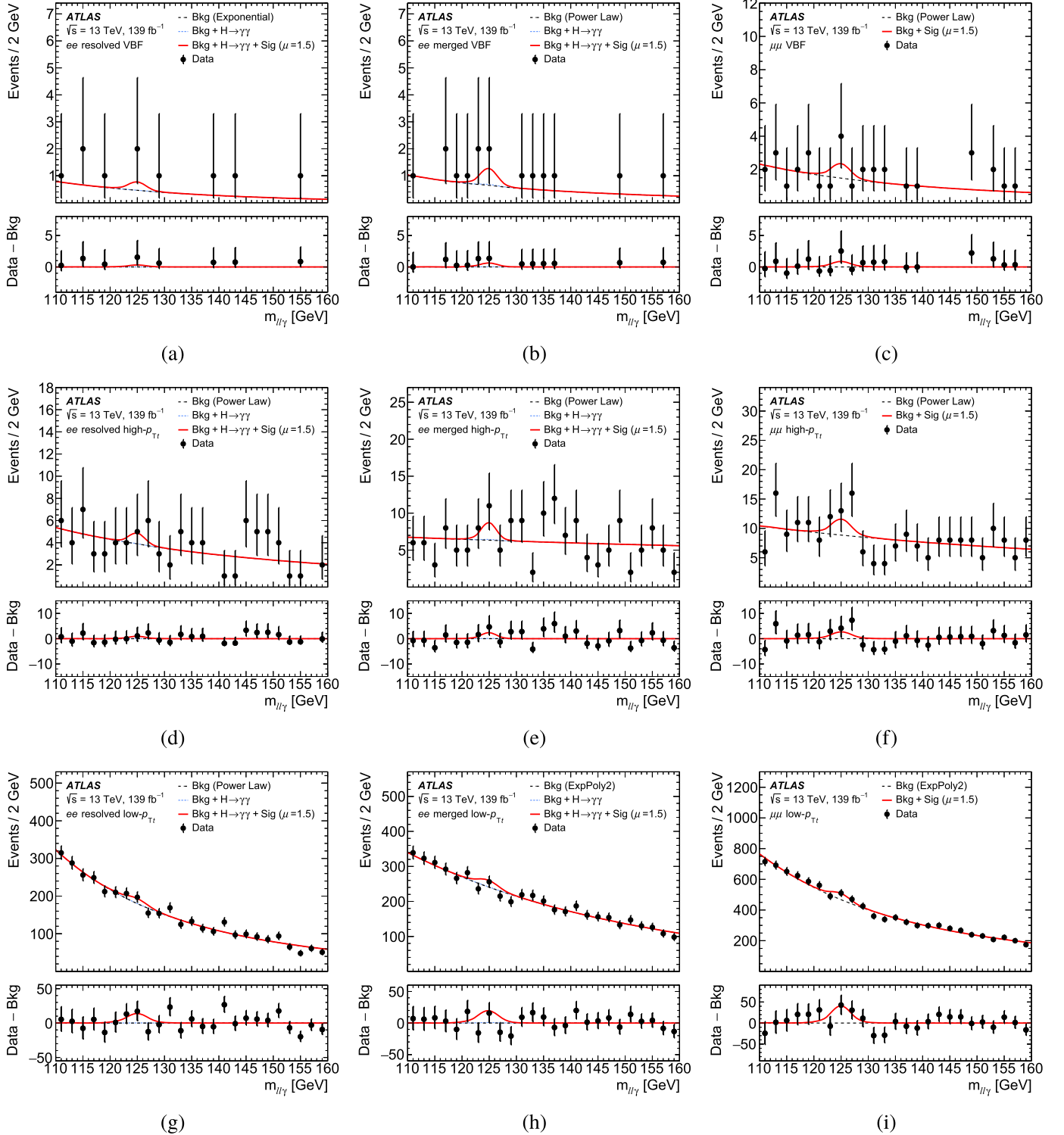


Fig. 3. $m_{\ell\ell\gamma}$ distributions of the selected events and the results of the global fit, for the VBF-enriched categories (a, b, c), the high- p_{Tl} categories (d, e, f), and the low- p_{Tl} categories (g, h, i). The ee -resolved categories are shown in the left column, the ee -merged categories in the middle and the $\mu\mu$ categories in the right column. The data are shown as the black circles with statistical uncertainties. The red curve shows the combined signal-plus-background model, the dashed black line shows the model of the non-resonant background component and the dotted blue line denotes the sum of the non-resonant background and the resonant $H \rightarrow \gamma\gamma$ background. The curves are obtained from the fit, i.e. they include the best-fit values of the parameter of interest and the nuisance parameters, including the spurious signal. The bottom panel shows the residuals of the data with respect to the non-resonant background of the signal-plus-background fit.

The observed (expected) significance over the background-only hypothesis for a Higgs boson with a mass of 125.09 GeV is 3.2σ (2.1σ).

The Higgs boson production cross-section times the $H \rightarrow \ell\ell\gamma$ branching ratio for $m_{\ell\ell} < 30$ GeV is determined to be $8.7^{+2.8}_{-2.7}$ fb = 8.7 ± 2.7 (stat.) $^{+0.7}_{-0.6}$ (syst.) fb.

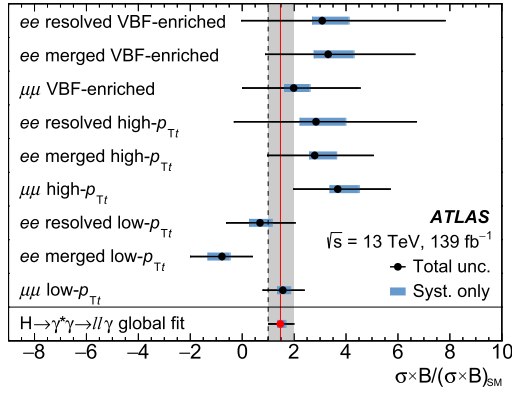


Fig. 4. Best-fit values of the signal-strength parameters for all event categories, in a fit where the signal strength in each category is allowed to float independently (black circles), compared with the result of the global fit (red circle and line) including its total uncertainty (grey band).

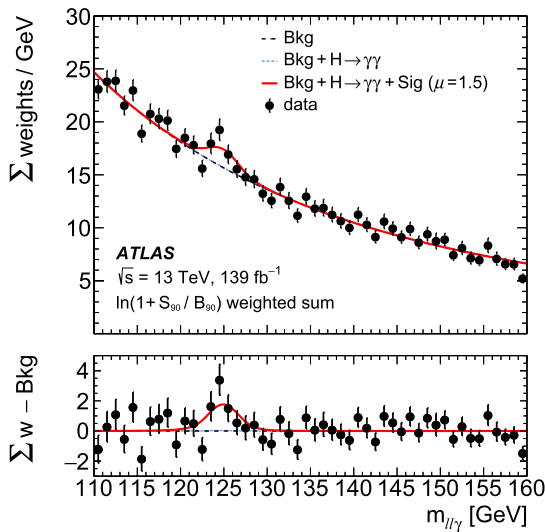


Fig. 5. $m_{\ell\ell\gamma}$ distribution, with every data event reweighted by a category-dependent weight, $\ln(1 + S_{90}/B_{90})$, where S_{90} is the number of signal events in the smallest window containing 90% of the expected signal, and B_{90} is the expected number of background events in the same window, estimated from fits to the data sidebands using the background models. The data are shown as the black circles with statistical uncertainties. The parameterised signal and backgrounds are also added up with the category-dependent weight. The red curve shows the combined signal-plus-background model when fitting all analysis categories simultaneously, the dashed black line shows the model of the non-resonant background component and the dotted blue line denotes the sum of the non-resonant background and the resonant $H \rightarrow \gamma\gamma$ background. The curves are obtained from the fit, i.e. they include the best-fit values of the parameter of interest and the nuisance parameters, including the spurious signal. The bottom panel shows the residuals of the data with respect to the non-resonant background component of the signal-plus-background fit.

9. Conclusion

A search for the Higgs boson decaying into a low-mass pair of electrons or muons and a photon is presented. The analysis is performed using a data set recorded by the ATLAS experiment at the LHC with proton–proton collisions at a centre-of-mass energy of 13 TeV, corresponding to an integrated luminosity of 139 fb^{-1} . For a Higgs boson with a mass of 125.09 GeV and $m_{\ell\ell} < 30 \text{ GeV}$, evidence for the $H \rightarrow \ell\ell\gamma$ process is found with a significance of 3.2σ over the background-only hypothesis, compared to an expected significance of 2.1σ . The best-fit value of the signal-strength parameter, defined as the ratio of the observed signal yield to the signal yield expected in the Standard Model, is $\mu = 1.5 \pm 0.5$. The Higgs boson production cross-section times the

$H \rightarrow \ell\ell\gamma$ branching ratio for $m_{\ell\ell} < 30 \text{ GeV}$ is determined to be $8.7_{-2.7}^{+2.8} \text{ fb}$. This result constitutes the first evidence for the decay of the Higgs boson into a pair of leptons and a photon, an important step towards probing Higgs boson couplings in this rare decay channel.

Declaration of competing interest

The authors declare that they have no known competing financial interests or personal relationships that could have appeared to influence the work reported in this paper.

Acknowledgements

We thank CERN for the very successful operation of the LHC, as well as the support staff from our institutions without whom ATLAS could not be operated efficiently.

We acknowledge the support of ANPCyT, Argentina; YerPhI, Armenia; ARC, Australia; BMWFW and FWF, Austria; ANAS, Azerbaijan; SSTC, Belarus; CNPq and FAPESP, Brazil; NSERC, NRC and CFI, Canada; CERN; ANID, Chile; CAS, MOST and NSFC, China; COLCIENCIAS, Colombia; MSMT CR, MPO CR and VSC CR, Czech Republic; DNRF and DNSRC, Denmark; IN2P3-CNRS and CEA-DRF/IRFU, France; SRNSFG, Georgia; BMBF, HGF and MPG, Germany; GSRT, Greece; RGC and Hong Kong SAR, China; ISF and Benozziyo Center, Israel; INFN, Italy; MEXT and JSPS, Japan; CNRST, Morocco; NWO, Netherlands; RCN, Norway; MNiSW and NCN, Poland; FCT, Portugal; MNE/IFA, Romania; JINR; MES of Russia and NRC KI, Russian Federation; MESTD, Serbia; MSSR, Slovakia; ARRS and MIZŠ, Slovenia; DST/NRF, South Africa; MICINN, Spain; SRC and Wallenberg Foundation, Sweden; SERI, SNSF and Cantons of Bern and Geneva, Switzerland; MOST, Taiwan; TAEK, Turkey; STFC, United Kingdom; DOE and NSF, United States of America. In addition, individual groups and members have received support from BCKDF, CANARIE, Compute Canada, CRC and IVADO, Canada; Beijing Municipal Science & Technology Commission, China; COST, ERC, ERDF, Horizon 2020 and Marie Skłodowska-Curie Actions, European Union; Investissements d’Avenir Labex, Investissements d’Avenir IDEX and ANR, France; DFG and AvH Foundation, Germany; Herakleitos, Thales and Aristeia programmes co-financed by EU-ESF and the Greek NSRF, Greece; BSF-NSF and GIF, Israel; La Caixa Banking Foundation, CERCA Programme Generalitat de Catalunya and PROMETEO and GenT Programmes Generalitat Valenciana, Spain; Göran Gustafssons Stiftelser, Sweden; The Royal Society and Leverhulme Trust, United Kingdom.

The crucial computing support from all WLCG partners is acknowledged gratefully, in particular from CERN, the ATLAS Tier-1 facilities at TRIUMF (Canada), NDGF (Denmark, Norway, Sweden), CC-IN2P3 (France), KIT/GridKA (Germany), INFN-CNAF (Italy), NL-T1 (Netherlands), PIC (Spain), ASGC (Taiwan), RAL (UK) and BNL (USA), the Tier-2 facilities worldwide and large non-WLCG resource providers. Major contributors of computing resources are listed in Ref. [97].

References

- [1] ATLAS Collaboration, Observation of a new particle in the search for the Standard Model Higgs boson with the ATLAS detector at the LHC, Phys. Lett. B 716 (2012) 1, arXiv:1207.7214 [hep-ex].
- [2] CMS Collaboration, Observation of a new boson at a mass of 125 GeV with the CMS experiment at the LHC, Phys. Lett. B 716 (2012) 30, arXiv:1207.7235 [hep-ex].
- [3] ATLAS Collaboration, Study of the spin and parity of the Higgs boson in diboson decays with the ATLAS detector, Eur. Phys. J. C 75 (2015) 476, arXiv:1506.05669 [hep-ex]; Erratum: Eur. Phys. J. C 76 (2016) 152.
- [4] CMS Collaboration, Constraints on the spin-parity and anomalous HVV couplings of the Higgs boson in proton collisions at 7 and 8 TeV, Phys. Rev. D 92 (2015) 012004, arXiv:1411.3441 [hep-ex].

- [5] ATLAS CMS Collaborations, Measurements of the Higgs boson production and decay rates and constraints on its couplings from a combined ATLAS and CMS analysis of the LHC pp collision data at $\sqrt{s} = 7$ and 8 TeV, *J. High Energy Phys.* 08 (2016) 045, arXiv:1606.02266 [hep-ex].
- [6] CMS Collaboration, Combined measurements of Higgs boson couplings in proton–proton collisions at $\sqrt{s} = 13$ TeV, *Eur. Phys. J. C* 79 (2019) 421, arXiv:1809.10733 [hep-ex].
- [7] ATLAS Collaboration, Combined measurements of Higgs boson production and decay using up to 80 fb⁻¹ of proton–proton collision data at $\sqrt{s} = 13$ TeV collected with the ATLAS experiment, *Phys. Rev. D* 101 (2020) 012002, arXiv:1909.02845 [hep-ex].
- [8] A. Kachanovich, U. Nierste, I. Nišandžić, Higgs boson decay into a lepton pair and a photon revisited, *Phys. Rev. D* 101 (2020) 073003, arXiv:2001.06516 [hep-ph].
- [9] A.Y. Korchin, V.A. Kovalchuk, Angular distribution and forward–backward asymmetry of the Higgs-boson decay to photon and lepton pair, *Eur. Phys. J. C* 74 (2014) 3141, arXiv:1408.0342 [hep-ph].
- [10] Y. Chen, A. Falkowski, I. Low, R. Vega-Morales, New observables for CP violation in Higgs decays, *Phys. Rev. D* 90 (2014) 113006, arXiv:1405.6723 [hep-ph].
- [11] L.-B. Chen, C.-F. Qiao, R.-L. Zhu, Reconstructing the 125 GeV SM Higgs boson through $\ell\bar{\ell}\gamma$, *Phys. Lett. B* 726 (2013) 306, arXiv:1211.6058 [hep-ph]; Erratum: *Phys. Lett. B* 808 (2020) 135629.
- [12] G. Passarino, Higgs boson production and decay: Dalitz sector, *Phys. Lett. B* 727 (2013) 424, arXiv:1308.0422 [hep-ph].
- [13] CMS Collaboration, Search for the decay of a Higgs boson in the $\ell\ell\gamma$ channel in proton–proton collisions at $\sqrt{s} = 13$ TeV, *J. High Energy Phys.* 11 (2018) 152, arXiv:1806.05996 [hep-ex].
- [14] ATLAS Collaboration, A search for the $Z\gamma$ decay mode of the Higgs boson in pp collisions at $\sqrt{s} = 13$ TeV with the ATLAS detector, *Phys. Lett. B* 809 (2020) 135754, arXiv:2005.05382 [hep-ex].
- [15] CMS Collaboration, Search for a Higgs boson decaying into $\gamma^*\gamma \rightarrow \ell\ell\gamma$ with low dilepton mass in pp collisions at $\sqrt{s} = 8$ TeV, *Phys. Lett. B* 753 (2016) 341, arXiv:1507.03031 [hep-ex].
- [16] ATLAS Collaboration, The ATLAS experiment at the CERN Large Hadron Collider, *J. Instrum.* 3 (2008) S08003.
- [17] ATLAS Collaboration, ATLAS insertable B-layer technical design report, ATLAS-TDR-19, <https://cds.cern.ch/record/1291633>, 2010; ATLAS insertable B-layer technical design report addendum, ATLAS-TDR-19-ADD-1, <https://cds.cern.ch/record/1451888>, 2012.
- [18] B. Abbott, et al., Production and integration of the ATLAS insertable B-layer, *J. Instrum.* 13 (2018) T05008, arXiv:1803.00844 [physics.ins-det].
- [19] ATLAS Collaboration, Electron and photon performance measurements with the ATLAS detector using the 2015–2017 LHC proton–proton collision data, *J. Instrum.* 14 (2019) P12006, arXiv:1908.00005 [hep-ex].
- [20] ATLAS Collaboration, Performance of the ATLAS trigger system in 2015, *Eur. Phys. J. C* 77 (2017) 317, arXiv:1611.09661 [hep-ex].
- [21] ATLAS Collaboration, ATLAS data quality operations and performance for 2015–2018 data-taking, *J. Instrum.* 15 (2020) P04003, arXiv:1911.04632 [physics.ins-det].
- [22] ATLAS Collaboration, Performance of electron and photon triggers in ATLAS during LHC Run 2, *Eur. Phys. J. C* 80 (2020) 47, arXiv:1909.00761 [hep-ex].
- [23] ATLAS Collaboration, The ATLAS simulation infrastructure, *Eur. Phys. J. C* 70 (2010) 823, arXiv:1005.4568 [physics.ins-det].
- [24] S. Agostinelli, et al., GEANT4 - a simulation toolkit, *Nucl. Instrum. Methods A* 506 (2003) 250.
- [25] T. Sjöstrand, S. Mrenna, P. Skands, A brief introduction to PYTHIA 8.1, *Comput. Phys. Commun.* 178 (2008) 852, arXiv:0710.3820 [hep-ph].
- [26] R.D. Ball, et al., Parton distributions with LHC data, *Nucl. Phys. B* 867 (2013) 244, arXiv:1207.1303 [hep-ph].
- [27] ATLAS Collaboration, The Pythia 8 A3 tune description of ATLAS minimum bias and inelastic measurements incorporating the Donnachie–Landshoff diffractive model, ATLAS-PHYS-PUB-2016-017, <https://cds.cern.ch/record/2206965>, 2016.
- [28] P. Nason, C. Oleari, NLO Higgs boson production via vector-boson fusion matched with shower in POWHEG, *J. High Energy Phys.* 02 (2010) 037, arXiv:0911.5299 [hep-ph].
- [29] S. Alioli, P. Nason, C. Oleari, E. Re, A general framework for implementing NLO calculations in shower Monte Carlo programs: the POWHEG BOX, *J. High Energy Phys.* 06 (2010) (using ATLAS svn revisions r2856 for v1, r3080 for v2 ggF, r3052 for v2 VBF, and r3133 for v2 VH) arXiv:1002.2581 [hep-ph].
- [30] P. Nason, A new method for combining NLO QCD with shower Monte Carlo algorithms, *J. High Energy Phys.* 11 (2004) 040, arXiv:hep-ph/0409146.
- [31] S. Frixione, P. Nason, C. Oleari, Matching NLO QCD computations with Parton Shower simulations: the POWHEG method, *J. High Energy Phys.* 11 (2007) 070, arXiv:0709.2092 [hep-ph].
- [32] H.B. Hartanto, B. Jager, L. Reina, D. Wackerth, Higgs boson production in association with top quarks in the POWHEG BOX, *Phys. Rev. D* 91 (2015) 094003, arXiv:1501.04498 [hep-ph].
- [33] J. Butterworth, et al., PDF4LHC recommendations for LHC Run II, *J. Phys. G* 43 (2016) 023001, arXiv:1510.03865 [hep-ph].
- [34] K. Hamilton, P. Nason, E. Re, G. Zanderighi, NNLOPS simulation of Higgs boson production, *J. High Energy Phys.* 10 (2013) 222, arXiv:1309.0017 [hep-ph].
- [35] K. Hamilton, P. Nason, G. Zanderighi, Finite quark-mass effects in the NNLOPS POWHEG+MiNLO Higgs generator, *J. High Energy Phys.* 05 (2015) 140, arXiv:1501.04637 [hep-ph].
- [36] S. Catani, M. Grazzini, Next-to-Next-to-Leading-Order Subtraction Formalism in Hadron Collisions and its Application to Higgs-boson Production at the Large Hadron Collider, *Phys. Rev. Lett.* 98 (2007) 222002, arXiv:hep-ph/0703012 [hep-ph].
- [37] G. Cullen, et al., Automated one-loop calculations with GoSam, *Eur. Phys. J. C* 72 (2012) 1889, arXiv:1111.2034 [hep-ph].
- [38] K. Hamilton, P. Nason, C. Oleari, G. Zanderighi, Merging H/W/Z + 0 and 1 jet at NLO with no merging scale: a path to parton shower + NNLO matching, *J. High Energy Phys.* 05 (2013) 082, arXiv:1212.4504 [hep-ph].
- [39] G. Luisoni, P. Nason, C. Oleari, F. Tramontano, $HW^\pm/HZ + 0$ and 1 jet at NLO with the POWHEG BOX interfaced to GoSam and their merging within MiNLO, *J. High Energy Phys.* 10 (2013) 083, arXiv:1306.2542 [hep-ph].
- [40] J. Bellm, et al., Herwig 7.0/Herwig++ 3.0 release note, *Eur. Phys. J. C* 76 (2016) 196, arXiv:1512.01178 [hep-ph].
- [41] D. de Florian, et al., Handbook of LHC Higgs cross sections: 4. Deciphering the nature of the Higgs sector, arXiv:1610.07922 [hep-ph], 2016.
- [42] ATLAS CMS Collaborations, Combined measurement of the Higgs boson mass in pp collisions at $\sqrt{s} = 7$ and 8 TeV with the ATLAS and CMS experiments, *Phys. Rev. Lett.* 114 (2015) 191803, arXiv:1503.07589 [hep-ex].
- [43] C. Anastasiou, C. Duhr, F. Dulat, F. Herzog, B. Mistlberger, Higgs boson gluon-fusion production in QCD at three loops, *Phys. Rev. Lett.* 114 (2015) 212001, arXiv:1503.06056 [hep-ph].
- [44] C. Anastasiou, et al., High precision determination of the gluon fusion Higgs boson cross-section at the LHC, *J. High Energy Phys.* 05 (2016) 058, arXiv:1602.00695 [hep-ph].
- [45] F. Dulat, A. Lazopoulos, B. Mistlberger, iHixs 2 - inclusive Higgs cross sections, *Comput. Phys. Commun.* 233 (2018) 243, arXiv:1802.00827 [hep-ph].
- [46] R.V. Harlander, K.J. Ozeren, Finite top mass effects for hadronic Higgs production at next-to-next-to-leading order, *J. High Energy Phys.* 11 (2009) 088, arXiv:0909.3420 [hep-ph].
- [47] R.V. Harlander, K.J. Ozeren, Top mass effects in Higgs production at next-to-next-to-leading order QCD: virtual corrections, *Phys. Lett. B* 679 (2009) 467, arXiv:0907.2997 [hep-ph].
- [48] R.V. Harlander, H. Mantler, S. Marzani, K.J. Ozeren, Higgs production in gluon fusion at next-to-next-to-leading order QCD for finite top mass, *Eur. Phys. J. C* 66 (2010) 359, arXiv:0912.2104 [hep-ph].
- [49] A. Pak, M. Rogal, M. Steinhauser, Finite top quark mass effects in NNLO Higgs boson production at LHC, *J. High Energy Phys.* 02 (2010) 025, arXiv:0911.4662 [hep-ph].
- [50] S. Actis, G. Passarino, C. Sturm, S. Uccirati, NLO electroweak corrections to Higgs boson production at hadron colliders, *Phys. Lett. B* 670 (2008) 12, arXiv:0809.1301 [hep-ph].
- [51] S. Actis, G. Passarino, C. Sturm, S. Uccirati, NNLO computational techniques: the cases $H \rightarrow \gamma\gamma$ and $H \rightarrow gg$, *Nucl. Phys. B* 811 (2009) 182, arXiv:0809.3667 [hep-ph].
- [52] C. Anastasiou, R. Boughezal, F. Petriello, Mixed QCD-electroweak corrections to Higgs boson production in gluon fusion, *J. High Energy Phys.* 04 (2009) 003, arXiv:0811.3458 [hep-ph].
- [53] U. Aglietti, R. Bonciani, G. Degrossi, A. Vicini, Two-loop light fermion contribution to Higgs production and decays, *Phys. Lett. B* 595 (2004) 432, arXiv:hep-ph/0404071 [hep-ph].
- [54] M. Bonetti, K. Melnikov, L. Tancredi, Higher order corrections to mixed QCD-EW contributions to Higgs boson production in gluon fusion, *Phys. Rev. D* 97 (2018) 056017; Erratum: *Phys. Rev. D* 97 (2018) 099906, arXiv:1801.10403 [hep-ph].
- [55] M. Ciccolini, A. Denner, S. Dittmaier, Strong and electroweak corrections to the production of a Higgs boson + 2 jets via weak interactions at the large hadron collider, *Phys. Rev. Lett.* 99 (2007) 161803, arXiv:0707.0381 [hep-ph].
- [56] M. Ciccolini, A. Denner, S. Dittmaier, Electroweak and QCD corrections to Higgs production via vector-boson fusion at the CERN LHC, *Phys. Rev. D* 77 (2008) 013002, arXiv:0710.4749 [hep-ph].
- [57] P. Bolzoni, F. Maltoni, S.-O. Moch, M. Zaro, Higgs boson production via vector-boson fusion at next-to-next-to-leading order in QCD, *Phys. Rev. Lett.* 105 (2010) 011801, arXiv:1003.4451 [hep-ph].
- [58] M.L. Ciccolini, S. Dittmaier, M. Krämer, Electroweak radiative corrections to associated WH and ZH production at hadron colliders, *Phys. Rev. D* 68 (2003) 073003, arXiv:hep-ph/0306234 [hep-ph].
- [59] O. Brein, A. Djouadi, R. Harlander, NNLO QCD corrections to the Higgs-strahlung processes at hadron colliders, *Phys. Lett. B* 579 (2004) 149, arXiv:hep-ph/0307206.
- [60] O. Brein, R. Harlander, M. Wiesemann, T. Zirke, Top-quark mediated effects in hadronic Higgs-Strahlung, *Eur. Phys. J. C* 72 (2012) 1868, arXiv:1111.0761 [hep-ph].
- [61] L. Altenkamp, S. Dittmaier, R.V. Harlander, H. Rzehak, T.J.E. Zirke, Gluon-induced Higgs-strahlung at next-to-leading order QCD, *J. High Energy Phys.* 02 (2013) 078, arXiv:1211.5015 [hep-ph].
- [62] A. Denner, S. Dittmaier, S. Kallweit, A. Mück, HAWK 2.0: a Monte Carlo program for Higgs production in vector-boson fusion and Higgs strahlung at hadron colliders, *Comput. Phys. Commun.* 195 (2015) 161, arXiv:1412.5390 [hep-ph].

- [63] O. Brein, R.V. Harlander, T.J.E. Zirke, *vh@nnlo* – Higgs Strahlung at hadron colliders, *Comput. Phys. Commun.* 184 (2013) 998, arXiv:1210.5347 [hep-ph].
- [64] R.V. Harlander, A. Kulesza, V. Theeuwes, T. Zirke, Soft gluon resummation for gluon-induced Higgs Strahlung, *J. High Energy Phys.* 11 (2014) 082, arXiv:1410.0217 [hep-ph].
- [65] R.V. Harlander, J. Klappert, S. Liebler, L. Simon, *vh@nnlo-v2*: new physics in Higgs Strahlung, *J. High Energy Phys.* 05 (2018) 089, arXiv:1802.04817 [hep-ph].
- [66] W. Beenakker, et al., NLO QCD corrections to $t\bar{t}H$ production in hadron collisions, *Nucl. Phys. B* 653 (2003) 151, arXiv:hep-ph/0211352.
- [67] S. Dawson, C. Jackson, L.H. Orr, L. Reina, D. Wackerth, Associated Higgs boson production with top quarks at the CERN large hadron collider: NLO QCD corrections, *Phys. Rev. D* 68 (2003) 034022, arXiv:hep-ph/0305087.
- [68] Y. Zhang, W.-G. Ma, R.-Y. Zhang, C. Chen, L. Guo, QCD NLO and EW NLO corrections to $t\bar{t}H$ production with top quark decays at hadron collider, *Phys. Lett. B* 738 (2014) 1, arXiv:1407.1110 [hep-ph].
- [69] S. Frixione, V. Hirschi, D. Pagani, H.-S. Shao, M. Zaro, Electroweak and QCD corrections to top-pair hadroproduction in association with heavy bosons, *J. High Energy Phys.* 06 (2015) 184, arXiv:1504.03446 [hep-ph].
- [70] S. Dawson, C. Jackson, L. Reina, D. Wackerth, Exclusive Higgs boson production with bottom quarks at hadron colliders, *Phys. Rev. D* 69 (2004) 074027, arXiv:hep-ph/0311067.
- [71] S. Dittmaier, M. Krämer, M. Spira, Higgs radiation off bottom quarks at the Fermilab Tevatron and the CERN LHC, *Phys. Rev. D* 70 (2004) 074010, arXiv:hep-ph/0309204.
- [72] R. Harlander, M. Kramer, M. Schumacher, Bottom-quark associated Higgs-boson production: reconciling the four- and five-flavour scheme approach, arXiv:1112.3478 [hep-ph], 2011.
- [73] A. Abbasabadi, D. Bowser-Chao, D.A. Dicus, W.W. Repko, Radiative Higgs boson decays $H \rightarrow f\bar{f}\gamma$, *Phys. Rev. D* 55 (1997) 5647, arXiv:hep-ph/9611209.
- [74] A. Firani, R. Stroynowski, Internal conversions in Higgs decays to two photons, *Phys. Rev. D* 76 (2007) 057301, arXiv:0704.3987 [hep-ph].
- [75] D.A. Dicus, W.W. Repko, Calculation of the decay $H \rightarrow e\bar{e}\gamma$, *Phys. Rev. D* 87 (2013) 077301, arXiv:1302.2159 [hep-ph].
- [76] D.A. Dicus, W.W. Repko, Dalitz decay $H \rightarrow f\bar{f}\gamma$ as a background for $H \rightarrow \gamma\gamma$, *Phys. Rev. D* 89 (2014) 093013, arXiv:1402.5317 [hep-ph].
- [77] E. Bothmann, et al., Event generation with Sherpa 2.2, *SciPost Phys.* 7 (2019) 034, arXiv:1905.09127 [hep-ph].
- [78] R.D. Ball, et al., Parton distributions for the LHC Run II, *J. High Energy Phys.* 04 (2015) 040, arXiv:1410.8849 [hep-ph].
- [79] ATLAS Collaboration, Muon reconstruction performance of the ATLAS detector in proton–proton collision data at $\sqrt{s} = 13$ TeV, *Eur. Phys. J. C* 76 (2016) 292, arXiv:1603.05598 [hep-ex].
- [80] ATLAS Collaboration, Muon reconstruction and identification efficiency in ATLAS using the full Run 2 pp collision data set at $\sqrt{s} = 13$ TeV, arXiv:2012.00578 [hep-ex], 2020.
- [81] ATLAS Collaboration, Measurement of the photon identification efficiencies with the ATLAS detector using LHC Run 2 data collected in 2015 and 2016, *Eur. Phys. J. C* 79 (2019) 205, arXiv:1810.05087 [hep-ex].
- [82] ATLAS Collaboration, Electron reconstruction and identification in the ATLAS experiment using the 2015 and 2016 LHC proton–proton collision data at $\sqrt{s} = 13$ TeV, *Eur. Phys. J. C* 79 (2019) 639, arXiv:1902.04655 [hep-ex].
- [83] R. Fruhwirth, Application of Kalman filtering to track and vertex fitting, *Nucl. Instrum. Methods A* 262 (1987) 444.
- [84] ATLAS Collaboration, Particle identification performance of the ATLAS transition radiation tracker, ATLAS-CONF-2011-128, <https://cds.cern.ch/record/1383793>, 2011.
- [85] ATLAS Collaboration, Topological cell clustering in the ATLAS calorimeters and its performance in LHC Run 1, *Eur. Phys. J. C* 77 (2017) 490, arXiv:1603.02934 [hep-ex].
- [86] M. Cacciari, G.P. Salam, G. Soyez, The anti- k_r jet clustering algorithm, *J. High Energy Phys.* 04 (2008) 063, arXiv:0802.1189 [hep-ph].
- [87] ATLAS Collaboration, Tagging and suppression of pileup jets with the ATLAS detector, ATLAS-CONF-2014-018, <https://cds.cern.ch/record/1700870>, 2014.
- [88] D.L. Rainwater, R. Szalapski, D. Zeppenfeld, Probing color singlet exchange in $Z + 2$ -jet events at the CERN LHC, *Phys. Rev. D* 54 (1996) 6680, arXiv:hep-ph/9605444.
- [89] OPAL Collaboration, Search for anomalous production of dilepton events with missing transverse momentum in e^+e^- collisions at $\sqrt{s} = 161$ GeV and 172 GeV, *Eur. Phys. J. C* 4 (1998) 47, arXiv:hep-ex/9710010.
- [90] M. Vesterinen, T. Wyatt, A novel technique for studying the Z boson transverse momentum distribution at hadron colliders, *Nucl. Instrum. Methods A* 602 (2009) 432, arXiv:0807.4956 [hep-ph].
- [91] M. Oreglia, A study of the reactions $\psi' \rightarrow \gamma\gamma\psi$, <https://www.slac.stanford.edu/cgi-wrap/getdoc/slac-r-236.pdf>, 1980.
- [92] ATLAS Collaboration, Search for scalar diphoton resonances in the mass range 65–600 GeV with the ATLAS detector in pp collision data at $\sqrt{s} = 8$ TeV, *Phys. Rev. Lett.* 113 (2014) 171801, arXiv:1407.6583 [hep-ex].
- [93] ATLAS Collaboration, Measurements of Higgs boson properties in the diphoton decay channel with 36 fb^{-1} of pp collision data at $\sqrt{s} = 13$ TeV with the ATLAS detector, *Phys. Rev. D* 98 (2018) 052005, arXiv:1802.04146 [hep-ex].
- [94] G. Cowan, K. Cranmer, E. Gross, O. Vitells, Asymptotic formulae for likelihood-based tests of new physics, *Eur. Phys. J. C* 71 (2011) 1554, arXiv:1007.1727 [physics.data-an]; Erratum: *Eur. Phys. J. C* 73 (2013) 2501.
- [95] ATLAS Collaboration, Luminosity determination in pp collisions at $\sqrt{s} = 13$ TeV using the ATLAS detector at the LHC, ATLAS-CONF-2019-021, <https://cds.cern.ch/record/2677054>, 2019.
- [96] G. Avoni, et al., The new LUCID-2 detector for luminosity measurement and monitoring in ATLAS, *J. Instrum.* 13 (2018) P07017.
- [97] ATLAS Collaboration, ATLAS computing acknowledgements, ATL-SOFT-PUB-2020-001, <https://cds.cern.ch/record/2717821>.

The ATLAS Collaboration

G. Aad¹⁰¹, B. Abbott¹²⁷, D.C. Abbott¹⁰², A. Abed Abud³⁶, K. Abeling⁵³, D.K. Abhayasinghe⁹³, S.H. Abidi²⁹, O.S. AbouZeid⁴⁰, N.L. Abraham¹⁵⁵, H. Abramowicz¹⁶⁰, H. Abreu¹⁵⁹, Y. Abulaiti⁶, A.C. Abusleme Hoffman^{145a}, B.S. Acharya^{66a,66b,p}, B. Achkar⁵³, L. Adam⁹⁹, C. Adam Bourdarios⁵, L. Adamczyk^{83a}, L. Adamek¹⁶⁵, J. Adelman¹²⁰, A. Adiguzel^{12c,ad}, S. Adorni⁵⁴, T. Adye¹⁴², A.A. Affolder¹⁴⁴, Y. Afik¹⁵⁹, C. Agapopoulou⁶⁴, M.N. Agaras³⁸, A. Aggarwal¹¹⁸, C. Agheorghiesei^{27c}, J.A. Aguilar-Saavedra^{138f,138a,ac}, A. Ahmad³⁶, F. Ahmadov⁷⁹, W.S. Ahmed¹⁰³, X. Ai⁴⁶, G. Aielli^{73a,73b}, S. Akatsuka⁸⁵, M. Akbiyik⁹⁹, T.P.A. Åkesson⁹⁶, E. Akilli⁵⁴, A.V. Akimov¹¹⁰, K. Al Khoury³⁹, G.L. Alberghi^{23b,23a}, J. Albert¹⁷⁴, M.J. Alconada Verzini¹⁶⁰, S. Alderweireldt³⁶, M. Aleksa³⁶, I.N. Aleksandrov⁷⁹, C. Alexa^{27b}, T. Alexopoulos¹⁰, A. Alfonsi¹¹⁹, F. Alfonsi^{23b,23a}, M. Alhroob¹²⁷, B. Ali¹⁴⁰, S. Ali¹⁵⁷, M. Aliev¹⁶⁴, G. Alimonti^{68a}, C. Allaire³⁶, B.M.M. Allbrooke¹⁵⁵, P.P. Allport²¹, A. Aloisio^{69a,69b}, F. Alonso⁸⁸, C. Alpigiani¹⁴⁷, E. Alunno Camelia^{73a,73b}, M. Alvarez Estevez⁹⁸, M.G. Alviggi^{69a,69b}, Y. Amaral Coutinho^{80b}, A. Ambler¹⁰³, L. Ambroz¹³³, C. Amelung³⁶, D. Amidei¹⁰⁵, S.P. Amor Dos Santos^{138a}, S. Amoroso⁴⁶, C.S. Amrouche⁵⁴, C. Anastopoulos¹⁴⁸, N. Andari¹⁴³, T. Andeen¹¹, J.K. Anders²⁰, S.Y. Andrean^{45a,45b}, A. Andreazza^{68a,68b}, V. Andrei^{61a}, S. Angelidakis⁹, A. Angerami³⁹, A.V. Anisenkov^{121b,121a}, A. Annovi^{71a}, C. Antel⁵⁴, M.T. Anthony¹⁴⁸, E. Antipov¹²⁸, M. Antonelli⁵¹, D.J.A. Antrim¹⁸, F. Anulli^{72a}, M. Aoki⁸¹, J.A. Aparisi Pozo¹⁷², M.A. Aparo¹⁵⁵, L. Aperio Bella⁴⁶, N. Aranzabal³⁶, V. Araujo Ferraz^{80a}, C. Arcangeletti⁵¹, A.T.H. Arce⁴⁹, E. Arena⁹⁰, J.-F. Arguin¹⁰⁹, S. Argyropoulos⁵², J.-H. Arling⁴⁶, A.J. Armbruster³⁶, A. Armstrong¹⁶⁹, O. Arnaez¹⁶⁵, H. Arnold³⁶, Z.P. Arrubarrena Tame¹¹³, G. Artoni¹³³, H. Asada¹¹⁶, K. Asai¹²⁵, S. Asai¹⁶², N.A. Asbah⁵⁹, E.M. Asimakopoulou¹⁷⁰, L. Asquith¹⁵⁵, J. Assahsah^{35e}, K. Assamagan²⁹, R. Astalos^{28a}, R.J. Atkin^{33a},

M. Atkinson¹⁷¹, N.B. Atlay¹⁹, H. Atmani⁶⁴, P.A. Atmasiddha¹⁰⁵, K. Augsten¹⁴⁰, V.A. Austrup¹⁸⁰,
 G. Avolio³⁶, M.K. Ayoub^{15c}, G. Azeleos^{109,ak}, D. Babal^{28a}, H. Bachacou¹⁴³, K. Bachas¹⁶¹,
 F. Backman^{45a,45b}, P. Bagnaia^{72a,72b}, M. Bahmani⁸⁴, H. Bahrasemani¹⁵¹, A.J. Bailey¹⁷², V.R. Bailey¹⁷¹,
 J.T. Baines¹⁴², C. Bakalis¹⁰, O.K. Baker¹⁸¹, P.J. Bakker¹¹⁹, E. Bakos¹⁶, D. Bakshi Gupta⁸, S. Balaji¹⁵⁶,
 R. Balasubramanian¹¹⁹, E.M. Baldin^{121b,121a}, P. Balek¹⁷⁸, E. Ballabene^{68a,68b}, F. Balli¹⁴³, W.K. Balunas¹³³,
 J. Balz⁹⁹, E. Banas⁸⁴, M. Bandieramonte¹³⁷, A. Bandyopadhyay¹⁹, L. Barak¹⁶⁰, W.M. Barbe³⁸,
 E.L. Barberio¹⁰⁴, D. Barberis^{55b,55a}, M. Barbero¹⁰¹, G. Barbour⁹⁴, K.N. Barends^{33a}, T. Barillari¹¹⁴,
 M-S. Barisits³⁶, J. Barkeloo¹³⁰, T. Barklow¹⁵², B.M. Barnett¹⁴², R.M. Barnett¹⁸, Z. Barnovska-Blenessy^{60a},
 A. Baroncelli^{60a}, G. Barone²⁹, A.J. Barr¹³³, L. Barranco Navarro^{45a,45b}, F. Barreiro⁹⁸,
 J. Barreiro Guimarães da Costa^{15a}, U. Barron¹⁶⁰, S. Barsov¹³⁶, F. Bartels^{61a}, R. Bartoldus¹⁵²,
 G. Bartolini¹⁰¹, A.E. Barton⁸⁹, P. Bartos^{28a}, A. Basalaev⁴⁶, A. Basan⁹⁹, I. Bashta^{74a,74b}, A. Bassalat^{64,ah},
 M.J. Basso¹⁶⁵, C.R. Basson¹⁰⁰, R.L. Bates⁵⁷, S. Batlamous^{35f}, J.R. Batley³², B. Batool¹⁵⁰, M. Battaglia¹⁴⁴,
 M. Bause^{72a,72b}, F. Bauer^{143,*}, P. Bauer²⁴, H.S. Bawa³¹, A. Bayirli^{12c}, J.B. Beacham⁴⁹, T. Beau¹³⁴,
 P.H. Beauchemin¹⁶⁸, F. Becherer⁵², P. Bechtel²⁴, H.P. Beck^{20,r}, K. Becker¹⁷⁶, C. Becot⁴⁶, A.J. Beddall^{12a},
 V.A. Bednyakov⁷⁹, C.P. Bee¹⁵⁴, T.A. Beermann¹⁸⁰, M. Begalli^{80b}, M. Begel²⁹, A. Behera¹⁵⁴, J.K. Behr⁴⁶,
 J.F. Beirer^{53,36}, F. Beisiegel²⁴, M. Belfkir⁵, G. Bella¹⁶⁰, L. Bellagamba^{23b}, A. Bellerive³⁴, P. Bellos²¹,
 K. Beloborodov^{121b,121a}, K. Belotskiy¹¹¹, N.L. Belyaev¹¹¹, D. Benckekroun^{35a}, Y. Benhammou¹⁶⁰,
 D.P. Benjamin⁶, M. Benoit²⁹, J.R. Bensinger²⁶, S. Bentvelsen¹¹⁹, L. Beresford¹³³, M. Beretta⁵¹,
 D. Berge¹⁹, E. Bergeaas Kuutmann¹⁷⁰, N. Berger⁵, B. Bergmann¹⁴⁰, L.J. Bergsten²⁶, J. Beringer¹⁸,
 S. Berlendis⁷, G. Bernardi¹³⁴, C. Bernius¹⁵², F.U. Bernlochner²⁴, T. Berry⁹³, P. Berta⁴⁶, A. Berthold⁴⁸,
 I.A. Bertram⁸⁹, O. Bessidskaia Bylund¹⁸⁰, S. Bethke¹¹⁴, A. Betti⁴², A.J. Bevan⁹², S. Bhatta¹⁵⁴,
 D.S. Bhattacharya¹⁷⁵, P. Bhattarai²⁶, V.S. Bhopatkar⁶, R. Bi¹³⁷, R.M. Bianchi¹³⁷, O. Biebel¹¹³, R. Bielski³⁶,
 K. Bierwagen⁹⁹, N.V. Biesuz^{71a,71b}, M. Biglietti^{74a}, T.R.V. Billoud¹⁴⁰, M. Bindi⁵³, A. Bingul^{12d},
 C. Bini^{72a,72b}, S. Biondi^{23b,23a}, C.J. Birch-sykes¹⁰⁰, G.A. Bird^{21,142}, M. Birman¹⁷⁸, T. Bisanz³⁶,
 J.P. Biswal³, D. Biswas^{179,k}, A. Bitadze¹⁰⁰, C. Bittrich⁴⁸, K. Bjørke¹³², T. Blazek^{28a}, I. Bloch⁴⁶,
 C. Blocker²⁶, A. Blue⁵⁷, U. Blumenschein⁹², G.J. Bobbink¹¹⁹, V.S. Bobrovnikov^{121b,121a}, D. Bogavac¹⁴,
 A.G. Bogdanchikov^{121b,121a}, C. Boehm^{45a}, V. Boisvert⁹³, P. Bokan⁴⁶, T. Bold^{83a}, M. Bomben¹³⁴,
 M. Bona⁹², M. Boonekamp¹⁴³, C.D. Booth⁹³, A.G. Borbély⁵⁷, H.M. Borecka-Bielska¹⁰⁹, L.S. Borgna⁹⁴,
 G. Borissov⁸⁹, D. Bortoletto¹³³, D. Boscherini^{23b}, M. Bosman¹⁴, J.D. Bossio Sola¹⁰³, K. Bouaouda^{35a},
 J. Boudreau¹³⁷, E.V. Bouhova-Thacker⁸⁹, D. Boumediene³⁸, R. Bouquet¹³⁴, A. Boveia¹²⁶, J. Boyd³⁶,
 D. Boye²⁹, I.R. Boyko⁷⁹, A.J. Bozson⁹³, J. Bracinik²¹, N. Brahimi^{60d,60c}, G. Brandt¹⁸⁰, O. Brandt³²,
 F. Braren⁴⁶, B. Brau¹⁰², J.E. Brau¹³⁰, W.D. Breaden Madden⁵⁷, K. Brendlinger⁴⁶, R. Brenner¹⁵⁹,
 L. Brenner³⁶, R. Brenner¹⁷⁰, S. Bressler¹⁷⁸, B. Brickwedde⁹⁹, D.L. Briglin²¹, D. Britton⁵⁷, D. Britzger¹¹⁴,
 I. Brock²⁴, R. Brock¹⁰⁶, G. Brooijmans³⁹, W.K. Brooks^{145d}, E. Brost²⁹, P.A. Bruckman de Renstrom⁸⁴,
 B. Brüers⁴⁶, D. Bruncko^{28b}, A. Bruni^{23b}, G. Bruni^{23b}, M. Bruschi^{23b}, N. Bruscinò^{72a,72b},
 L. Bryngemark¹⁵², T. Buanes¹⁷, Q. Buat¹⁵⁴, P. Buchholz¹⁵⁰, A.G. Buckley⁵⁷, I.A. Budagov⁷⁹,
 M.K. Bugge¹³², O. Bulekov¹¹¹, B.A. Bullard⁵⁹, T.J. Burch¹²⁰, S. Burdin⁹⁰, C.D. Burgard⁴⁶, A.M. Burger¹²⁸,
 B. Burghgrave⁸, J.T.P. Burr⁴⁶, C.D. Burton¹¹, J.C. Burzynski¹⁰², V. Büscher⁹⁹, E. Buschmann⁵³,
 P.J. Bussey⁵⁷, J.M. Butler²⁵, C.M. Buttar⁵⁷, J.M. Butterworth⁹⁴, W. Buttinger¹⁴², C.J. Buxo Vazquez¹⁰⁶,
 A.R. Buzykaev^{121b,121a}, G. Cabras^{23b,23a}, S. Cabrera Urbán¹⁷², D. Caforio⁵⁶, H. Cai¹³⁷, V.M.M. Cairo¹⁵²,
 O. Cakir^{4a}, N. Calace³⁶, P. Calafiura¹⁸, G. Calderini¹³⁴, P. Calfayan⁶⁵, G. Callea⁵⁷, L.P. Caloba^{80b},
 A. Caltabiano^{73a,73b}, S. Calvente Lopez⁹⁸, D. Calvet³⁸, S. Calvet³⁸, T.P. Calvet¹⁰¹, M. Calvetti^{71a,71b},
 R. Camacho Toro¹³⁴, S. Camarda³⁶, D. Camarero Munoz⁹⁸, P. Camarri^{73a,73b}, M.T. Camerlingo^{74a,74b},
 D. Cameron¹³², C. Camincher³⁶, M. Campanelli⁹⁴, A. Camplani⁴⁰, V. Canale^{69a,69b}, A. Canesse¹⁰³,
 M. Cano Bret⁷⁷, J. Cantero¹²⁸, Y. Cao¹⁷¹, M. Capua^{41b,41a}, R. Cardarelli^{73a}, F. Cardillo¹⁷²,
 G. Carducci^{41b,41a}, T. Carli³⁶, G. Carlino^{69a}, B.T. Carlson¹³⁷, E.M. Carlson^{174,166a}, L. Carminati^{68a,68b},
 M. Carnesale^{72a,72b}, R.M.D. Carney¹⁵², S. Caron¹¹⁸, E. Carquin^{145d}, S. Carrá⁴⁶, G. Carratta^{23b,23a},
 J.W.S. Carter¹⁶⁵, T.M. Carter⁵⁰, D. Casadei^{33c}, M.P. Casado^{14,h}, A.F. Casha¹⁶⁵, E.G. Castiglia¹⁸¹,
 F.L. Castillo¹⁷², L. Castillo Garcia¹⁴, V. Castillo Gimenez¹⁷², N.F. Castro^{138a,138e}, A. Catinaccio³⁶,
 J.R. Catmore¹³², A. Cattai³⁶, V. Cavaliere²⁹, N. Cavalli^{23b,23a}, V. Cavasinni^{71a,71b}, E. Celebi^{12b}, F. Celli¹³³,
 K. Cerny¹²⁹, A.S. Cerqueira^{80a}, A. Cerri¹⁵⁵, L. Cerrito^{73a,73b}, F. Cerutti¹⁸, A. Cervelli^{23b,23a}, S.A. Cetin^{12b},
 Z. Chadi^{35a}, D. Chakraborty¹²⁰, M. Chala^{138f}, J. Chan¹⁷⁹, W.S. Chan¹¹⁹, W.Y. Chan⁹⁰, J.D. Chapman³²,
 B. Chargeishvili^{158b}, D.G. Charlton²¹, T.P. Charman⁹², M. Chatterjee²⁰, C.C. Chau³⁴, S. Chekanov⁶,

S.V. Chekulaev^{166a}, G.A. Chelkov^{79.af}, B. Chen⁷⁸, C. Chen^{60a}, C.H. Chen⁷⁸, H. Chen^{15c}, H. Chen²⁹, J. Chen^{60a}, J. Chen³⁹, J. Chen²⁶, S. Chen¹³⁵, S.J. Chen^{15c}, X. Chen^{15b}, Y. Chen^{60a}, Y.-H. Chen⁴⁶, C.L. Cheng¹⁷⁹, H.C. Cheng^{62a}, H.J. Cheng^{15a}, A. Cheplakov⁷⁹, E. Cheremushkina⁴⁶, R. Cherkaoui El Moursli^{35f}, E. Cheu⁷, K. Cheung⁶³, L. Chevalier¹⁴³, V. Chiarella⁵¹, G. Chiarelli^{71a}, G. Chiodini^{67a}, A.S. Chisholm²¹, A. Chitan^{27b}, I. Chiu¹⁶², Y.H. Chiu¹⁷⁴, M.V. Chizhov^{79.t}, K. Choi¹¹, A.R. Chomont^{72a,72b}, Y. Chou¹⁰², Y.S. Chow¹¹⁹, L.D. Christopher^{33f}, M.C. Chu^{62a}, X. Chu^{15a,15d}, J. Chudoba¹³⁹, J.J. Chwastowski⁸⁴, D. Cieri¹¹⁴, K.M. Ciesla⁸⁴, V. Cindro⁹¹, I.A. Cioară^{27b}, A. Ciocio¹⁸, F. Ciotto^{69a,69b}, Z.H. Citron^{178.l}, M. Citterio^{68a}, D.A. Ciubotaru^{27b}, B.M. Ciungu¹⁶⁵, A. Clark⁵⁴, P.J. Clark⁵⁰, S.E. Clawson¹⁰⁰, C. Clement^{45a,45b}, L. Clissa^{23b,23a}, Y. Coadou¹⁰¹, M. Cobal^{66a,66c}, A. Coccaro^{55b}, J. Cochran⁷⁸, R. Coelho Lopes De Sa¹⁰², S. Coelli^{68a}, H. Cohen¹⁶⁰, A.E.C. Coimbra³⁶, B. Cole³⁹, J. Collot⁵⁸, P. Conde Muiño^{138a,138h}, S.H. Connell^{33c}, I.A. Connelly⁵⁷, E.I. Conroy¹³³, F. Conventi^{69a,al}, A.M. Cooper-Sarkar¹³³, F. Cormier¹⁷³, L.D. Corpe⁹⁴, M. Corradi^{72a,72b}, E.E. Corrigan⁹⁶, F. Corriveau^{103,aa}, M.J. Costa¹⁷², F. Costanza⁵, D. Costanzo¹⁴⁸, B.M. Cote¹²⁶, G. Cowan⁹³, J.W. Cowley³², J. Crane¹⁰⁰, K. Cranmer¹²⁴, R.A. Creager¹³⁵, S. Crépe-Renaudin⁵⁸, F. Crescioli¹³⁴, M. Cristinziani¹⁵⁰, M. Cristoforetti^{75a,75b,b}, V. Croft¹⁶⁸, G. Crosetti^{41b,41a}, A. Cueto⁵, T. Cuhadar Donszelmann¹⁶⁹, H. Cui^{15a,15d}, A.R. Cukierman¹⁵², W.R. Cunningham⁵⁷, S. Czekierda⁸⁴, P. Czodrowski³⁶, M.M. Czurylo^{61b}, M.J. Da Cunha Sargedas De Sousa^{60b}, J.V. Da Fonseca Pinto^{80b}, C. Da Via¹⁰⁰, W. Dabrowski^{83a}, T. Dado⁴⁷, S. Dahbi^{33f}, T. Dai¹⁰⁵, C. Dallapiccola¹⁰², M. Dam⁴⁰, G. D'amen²⁹, V. D'Amico^{74a,74b}, J. Damp⁹⁹, J.R. Dandoy¹³⁵, M.F. Daneri³⁰, M. Danninger¹⁵¹, V. Dao³⁶, G. Darbo^{55b}, A. Dattagupta¹³⁰, S. D'Auria^{68a,68b}, C. David^{166b}, T. Davidek¹⁴¹, D.R. Davis⁴⁹, B.R. Davis-purcell³⁴, I. Dawson⁹², K. De⁸, R. De Asmundis^{69a}, M. De Beurs¹¹⁹, S. De Castro^{23b,23a}, N. De Groot¹¹⁸, P. de Jong¹¹⁹, H. De la Torre¹⁰⁶, A. De Maria^{15c}, D. De Pedis^{72a}, A. De Salvo^{72a}, U. De Sanctis^{73a,73b}, M. De Santis^{73a,73b}, A. De Santo¹⁵⁵, J.B. De Vivie De Regie⁵⁸, D.V. Dedovich⁷⁹, J. Degens¹¹⁹, A.M. Deiana⁴², J. Del Peso⁹⁸, Y. Delabat Diaz⁴⁶, F. Deliot¹⁴³, C.M. Delitzsch⁷, M. Della Pietra^{69a,69b}, D. Della Volpe⁵⁴, A. Dell'Acqua³⁶, L. Dell'Asta^{73a,73b}, M. Delmastro⁵, P.A. Delsart⁵⁸, S. Demers¹⁸¹, M. Demichev⁷⁹, G. Demontigny¹⁰⁹, S.P. Denisov¹²², L. D'Eramo¹²⁰, D. Derendarz⁸⁴, J.E. Derkaoui^{35e}, F. Derue¹³⁴, P. Dervan⁹⁰, K. Desch²⁴, K. Dette¹⁶⁵, C. Deutsch²⁴, P.O. Deviveiros³⁶, F.A. Di Bello^{72a,72b}, A. Di Ciaccio^{73a,73b}, L. Di Ciaccio⁵, C. Di Donato^{69a,69b}, A. Di Girolamo³⁶, G. Di Gregorio^{71a,71b}, A. Di Luca^{75a,75b}, B. Di Micco^{74a,74b}, R. Di Nardo^{74a,74b}, C. Diaconu¹⁰¹, F.A. Dias¹¹⁹, T. Dias Do Vale^{138a}, M.A. Diaz^{145a}, F.G. Diaz Capriles²⁴, J. Dickinson¹⁸, M. Didenko¹⁶⁴, E.B. Diehl¹⁰⁵, J. Dietrich¹⁹, S. Díez Cornell⁴⁶, C. Diez Pardos¹⁵⁰, A. Dimitrievska¹⁸, W. Ding^{15b}, J. Dingfelder²⁴, S.J. Dittmeier^{61b}, F. Dittus³⁶, F. Djama¹⁰¹, T. Djobava^{158b}, J.I. Djuvsland¹⁷, M.A.B. Do Vale¹⁴⁶, M. Dobre^{27b}, D. Dodsworth²⁶, C. Doglioni⁹⁶, J. Dolejsi¹⁴¹, Z. Dolezal¹⁴¹, M. Donadelli^{80c}, B. Dong^{60c}, J. Donini³⁸, A. D'onofrio^{15c}, M. D'Onofrio⁹⁰, J. Dopke¹⁴², A. Doria^{69a}, M.T. Dova⁸⁸, A.T. Doyle⁵⁷, E. Drechsler¹⁵¹, E. Dreyer¹⁵¹, T. Dreyer⁵³, A.S. Drobac¹⁶⁸, D. Du^{60b}, T.A. du Pree¹¹⁹, Y. Duan^{60d}, F. Dubinin¹¹⁰, M. Dubovsky^{28a}, A. Dubreuil⁵⁴, E. Duchovni¹⁷⁸, G. Duckeck¹¹³, O.A. Ducu^{36,27b}, D. Duda¹¹⁴, A. Dudarev³⁶, A.C. Dudder⁹⁹, M. D'uffizi¹⁰⁰, L. Duflot⁶⁴, M. Dührssen³⁶, C. Dülsen¹⁸⁰, M. Dumancic¹⁷⁸, A.E. Dumitriu^{27b}, M. Dunford^{61a}, S. Dungs⁴⁷, A. Duperrin¹⁰¹, H. Duran Yildiz^{4a}, M. Düren⁵⁶, A. Durglishvili^{158b}, B. Dutta⁴⁶, D. Duvnjak¹, G.I. Dyckes¹³⁵, M. Dyndal^{83a}, S. Dysch¹⁰⁰, B.S. Dziedzic⁸⁴, B. Eckerova^{28a}, M.G. Eggleston⁴⁹, E. Egidio Purcino De Souza^{80b}, L.F. Ehrke⁵⁴, T. Eifert⁸, G. Eigen¹⁷, K. Einsweiler¹⁸, T. Ekelof¹⁷⁰, H. El Jarrari^{35f}, A. El Moussaouy^{35a}, V. Ellajosyula¹⁷⁰, M. Ellert¹⁷⁰, F. Ellinghaus¹⁸⁰, A.A. Elliot⁹², N. Ellis³⁶, J. Elmsheuser²⁹, M. Elsing³⁶, D. Emeliyanov¹⁴², A. Emerman³⁹, Y. Enari¹⁶², J. Erdmann⁴⁷, A. Ereditato²⁰, P.A. Erland⁸⁴, M. Errenst¹⁸⁰, M. Escalier⁶⁴, C. Escobar¹⁷², O. Estrada Pastor¹⁷², E. Etzion¹⁶⁰, G. Evans^{138a}, H. Evans⁶⁵, M.O. Evans¹⁵⁵, A. Ezhilov¹³⁶, F. Fabbri⁵⁷, L. Fabbri^{23b,23a}, V. Fabiani¹¹⁸, G. Facini¹⁷⁶, R.M. Fakhruddinov¹²², S. Falciano^{72a}, P.J. Falke²⁴, S. Falke³⁶, J. Faltova¹⁴¹, Y. Fan^{15a}, Y. Fang^{15a}, Y. Fang^{15a}, G. Fanourakis⁴⁴, M. Fanti^{68a,68b}, M. Faraj^{60c}, A. Farbin⁸, A. Farilla^{74a}, E.M. Farina^{70a,70b}, T. Farooque¹⁰⁶, S.M. Farrington⁵⁰, P. Farthouat³⁶, F. Fassi^{35f}, D. Fassouliotis⁹, M. Fauci Giannelli^{73a,73b}, W.J. Fawcett³², L. Fayard⁶⁴, O.L. Fedin^{136,q}, A. Fehr²⁰, M. Feickert¹⁷¹, L. Feligioni¹⁰¹, A. Fell¹⁴⁸, C. Feng^{60b}, M. Feng⁴⁹, M.J. Fenton¹⁶⁹, A.B. Fenyuk¹²², S.W. Ferguson⁴³, J. Ferrando⁴⁶, A. Ferrari¹⁷⁰, P. Ferrari¹¹⁹, R. Ferrari^{70a}, D. Ferrere⁵⁴, C. Ferretti¹⁰⁵, F. Fiedler⁹⁹, A. Filipčič⁹¹, F. Filthaut¹¹⁸, K.D. Finelli²⁵, M.C.N. Fiolhais^{138a,138c,a}, L. Fiorini¹⁷², F. Fischer¹¹³, J. Fischer⁹⁹, W.C. Fisher¹⁰⁶, T. Fitschen²¹, I. Fleck¹⁵⁰, P. Fleischmann¹⁰⁵, T. Flick¹⁸⁰, B.M. Flierl¹¹³, L. Flores¹³⁵, L.R. Flores Castillo^{62a}, F.M. Follega^{75a,75b}, N. Fomin¹⁷, J.H. Foo¹⁶⁵,

G.T. Forcolin^{75a,75b}, B.C. Forland⁶⁵, A. Formica¹⁴³, F.A. Förster¹⁴, A.C. Forti¹⁰⁰, E. Fortin¹⁰¹, M.G. Foti¹³³, D. Fournier⁶⁴, H. Fox⁸⁹, P. Francavilla^{71a,71b}, S. Francescato^{72a,72b}, M. Franchini^{23b,23a}, S. Franchino^{61a}, D. Francis³⁶, L. Franco⁵, L. Franconi²⁰, M. Franklin⁵⁹, G. Frattari^{72a,72b}, P.M. Freeman²¹, B. Freund¹⁰⁹, W.S. Freund^{80b}, E.M. Freundlich⁴⁷, D.C. Frizzell¹²⁷, D. Froidevaux³⁶, J.A. Frost¹³³, Y. Fu^{60a}, M. Fujimoto¹²⁵, E. Fullana Torregrosa¹⁷², T. Fusayasu¹¹⁵, J. Fuster¹⁷², A. Gabrielli^{23b,23a}, A. Gabrielli³⁶, P. Gadow⁴⁶, G. Gagliardi^{55b,55a}, L.G. Gagnon¹⁸, G.E. Gallardo¹³³, E.J. Gallas¹³³, B.J. Gallop¹⁴², R. Gamboa Goni⁹², K.K. Gan¹²⁶, S. Ganguly¹⁷⁸, J. Gao^{60a}, Y. Gao⁵⁰, Y.S. Gao^{31,n}, F.M. Garay Walls^{145a}, C. García¹⁷², J.E. García Navarro¹⁷², J.A. García Pascual^{15a}, M. Garcia-Sciveres¹⁸, R.W. Gardner³⁷, D. Garg⁷⁷, S. Gargiulo⁵², C.A. Garner¹⁶⁵, V. Garonne¹³², S.J. Gasiorowski¹⁴⁷, P. Gaspar^{80b}, G. Gaudio^{70a}, P. Gauzzi^{72a,72b}, I.L. Gavrilenko¹¹⁰, A. Gavrilyuk¹²³, C. Gay¹⁷³, G. Gaycken⁴⁶, E.N. Gazis¹⁰, A.A. Geanta^{27b}, C.M. Gee¹⁴⁴, C.N.P. Gee¹⁴², J. Geisen⁹⁶, M. Geisen⁹⁹, C. Gemme^{55b}, M.H. Genest⁵⁸, C. Geng¹⁰⁵, S. Gentile^{72a,72b}, S. George⁹³, T. Gerialis⁴⁴, L.O. Gerlach⁵³, P. Gessinger-Befurt⁹⁹, G. Gessner⁴⁷, M. Ghasemi Bostanabad¹⁷⁴, M. Ghneimat¹⁵⁰, A. Ghosh¹⁶⁹, A. Ghosh⁷⁷, B. Giacobbe^{23b}, S. Giagu^{72a,72b}, N. Giangiacomi¹⁶⁵, P. Giannetti^{71a}, A. Giannini^{69a,69b}, S.M. Gibson⁹³, M. Gignac¹⁴⁴, D.T. Gil^{83b}, B.J. Gilbert³⁹, D. Gillberg³⁴, G. Gilles¹⁸⁰, N.E.K. Gillwald⁴⁶, D.M. Gingrich^{3,ak}, M.P. Giordani^{66a,66c}, P.F. Giraud¹⁴³, G. Giugliarelli^{66a,66c}, D. Giugni^{68a}, F. Giuli^{73a,73b}, S. Gkaitatzis¹⁶¹, I. Gkialas^{9,i}, E.L. Gkougkousis¹⁴, P. Gkoutoumis¹⁰, L.K. Gladilin¹¹², C. Glasman⁹⁸, G.R. Gledhill¹³⁰, M. Glisic¹³⁰, I. Gnesi^{41b,d}, M. Goblirsch-Kolb²⁶, D. Godin¹⁰⁹, S. Goldfarb¹⁰⁴, T. Golling⁵⁴, D. Golubkov¹²², A. Gomes^{138a,138b}, R. Goncalves Gama⁵³, R. Gonçalves^{138a,138c}, G. Gonella¹³⁰, L. Gonella²¹, A. Gongadze⁷⁹, F. Gonnella²¹, J.L. Gonski³⁹, S. González de la Hoz¹⁷², S. Gonzalez Fernandez¹⁴, R. Gonzalez Lopez⁹⁰, C. Gonzalez Renteria¹⁸, R. Gonzalez Suarez¹⁷⁰, S. Gonzalez-Sevilla⁵⁴, G.R. Gonzalvo Rodriguez¹⁷², R.Y. González Andana^{145a}, L. Goossens³⁶, N.A. Gorasia²¹, P.A. Gorbounov¹²³, H.A. Gordon²⁹, B. Gorini³⁶, E. Gorini^{67a,67b}, A. Gorišek⁹¹, A.T. Goshaw⁴⁹, M.I. Gostkin⁷⁹, C.A. Gottardo¹¹⁸, M. Gouighri^{35b}, V. Goumarre⁴⁶, A.G. Goussiou¹⁴⁷, N. Govender^{33c}, C. Goy⁵, I. Grabowska-Bold^{83a}, K. Graham³⁴, E. Gramstad¹³², S. Grancagnolo¹⁹, M. Grandi¹⁵⁵, V. Gratchev¹³⁶, P.M. Gravila^{27f}, F.G. Gravili^{67a,67b}, H.M. Gray¹⁸, C. Grefe²⁴, I.M. Gregor⁴⁶, P. Grenier¹⁵², K. Grevtsov⁴⁶, C. Grieco¹⁴, N.A. Grieser¹²⁷, A.A. Grillo¹⁴⁴, K. Grimm^{31,m}, S. Grinstein^{14,x}, J.-F. Grivaz⁶⁴, S. Groh⁹⁹, E. Gross¹⁷⁸, J. Grosse-Knetter⁵³, Z.J. Grout⁹⁴, C. Grud¹⁰⁵, A. Grummer¹¹⁷, J.C. Grundy¹³³, L. Guan¹⁰⁵, W. Guan¹⁷⁹, C. Gubbels¹⁷³, J. Guenther³⁶, J.G.R. Guerrero Rojas¹⁷², F. Guescini¹¹⁴, D. Guest¹⁹, R. Gugel⁹⁹, A. Guida⁴⁶, T. Guillemin⁵, S. Guindon³⁶, J. Guo^{60c}, L. Guo⁶⁴, Y. Guo¹⁰⁵, R. Gupta⁴⁶, S. Gurbuz²⁴, G. Gustavino¹²⁷, M. Guth⁵², P. Gutierrez¹²⁷, L.F. Gutierrez Zagazeta¹³⁵, C. Gutschow⁹⁴, C. Guyot¹⁴³, C. Gwenlan¹³³, C.B. Gwilliam⁹⁰, E.S. Haaland¹³², A. Haas¹²⁴, M.H. Habedank¹⁹, C. Haber¹⁸, H.K. Hadavand⁸, A. Hadeef⁹⁹, M. Haleem¹⁷⁵, J. Haley¹²⁸, J.J. Hall¹⁴⁸, G. Halladjian¹⁰⁶, G.D. Hallewell¹⁰¹, L. Halser²⁰, K. Hamano¹⁷⁴, H. Hamdaoui^{35f}, M. Hamer²⁴, G.N. Hamity⁵⁰, K. Han^{60a}, L. Han^{15c}, L. Han^{60a}, S. Han¹⁸, Y.F. Han¹⁶⁵, K. Hanagaki^{81,v}, M. Hance¹⁴⁴, M.D. Hank³⁷, R. Hankache¹⁰⁰, E. Hansen⁹⁶, J.B. Hansen⁴⁰, J.D. Hansen⁴⁰, M.C. Hansen²⁴, P.H. Hansen⁴⁰, E.C. Hanson¹⁰⁰, K. Hara¹⁶⁷, T. Harenberg¹⁸⁰, S. Harkusha¹⁰⁷, Y.T. Harris¹³³, P.F. Harrison¹⁷⁶, N.M. Hartman¹⁵², N.M. Hartmann¹¹³, Y. Hasegawa¹⁴⁹, A. Hasib⁵⁰, S. Hassani¹⁴³, S. Haug²⁰, R. Hauser¹⁰⁶, M. Havranek¹⁴⁰, C.M. Hawkes²¹, R.J. Hawkins³⁶, S. Hayashida¹¹⁶, D. Hayden¹⁰⁶, C. Hayes¹⁰⁵, R.L. Hayes¹⁷³, C.P. Hays¹³³, J.M. Hays⁹², H.S. Hayward⁹⁰, S.J. Haywood¹⁴², F. He^{60a}, Y. He¹⁶³, Y. He¹³⁴, M.P. Heath⁵⁰, V. Hedberg⁹⁶, A.L. Heggelund¹³², N.D. Hehir⁹², C. Heidegger⁵², K.K. Heidegger⁵², W.D. Heidorn⁷⁸, J. Heilman³⁴, S. Heim⁴⁶, T. Heim¹⁸, B. Heinemann^{46,ai}, J.G. Heinlein¹³⁵, J.J. Heinrich¹³⁰, L. Heinrich³⁶, J. Hejbal¹³⁹, L. Helary⁴⁶, A. Held¹²⁴, S. Hellesund¹³², C.M. Helling¹⁴⁴, S. Hellman^{45a,45b}, C. Helsens³⁶, R.C.W. Henderson⁸⁹, L. Henkelmann³², A.M. Henriques Correia³⁶, H. Herde¹⁵², Y. Hernández Jiménez^{33f}, H. Herr⁹⁹, M.G. Herrmann¹¹³, T. Herrmann⁴⁸, G. Herten⁵², R. Hertenberger¹¹³, L. Hervas³⁶, N.P. Hessey^{166a}, H. Hibi⁸², S. Higashino⁸¹, E. Higón-Rodríguez¹⁷², K. Hildebrand³⁷, K.K. Hill²⁹, K.H. Hiller⁴⁶, S.J. Hillier²¹, M. Hils⁴⁸, I. Hinchliffe¹⁸, F. Hinterkeuser²⁴, M. Hirose¹³¹, S. Hirose¹⁶⁷, D. Hirschbuehl¹⁸⁰, B. Hiti⁹¹, O. Hladik¹³⁹, J. Hobbs¹⁵⁴, R. Hobincu^{27e}, N. Hod¹⁷⁸, M.C. Hodgkinson¹⁴⁸, B.H. Hodgkinson³², A. Hoecker³⁶, J. Hofer⁴⁶, D. Hohn⁵², T. Holm²⁴, T.R. Holmes³⁷, M. Holzbock¹¹⁴, L.B.A.H. Hommels³², B.P. Honan¹⁰⁰, T.M. Hong¹³⁷, J.C. Honig⁵², A. Hönle¹¹⁴, B.H. Hooberman¹⁷¹, W.H. Hopkins⁶, Y. Horii¹¹⁶, P. Horn⁴⁸, L.A. Horyn³⁷, S. Hou¹⁵⁷, J. Howarth⁵⁷, J. Hoya⁸⁸, M. Hrabovsky¹²⁹, A. Hrynevich¹⁰⁸, T. Hryn'ova⁵, P.J. Hsu⁶³, S.-C. Hsu¹⁴⁷, Q. Hu³⁹, S. Hu^{60c}, Y.F. Hu^{15a,15d,am}, D.P. Huang⁹⁴, X. Huang^{15c},

Y. Huang^{60a}, Y. Huang^{15a}, Z. Hubacek¹⁴⁰, F. Hubaut¹⁰¹, M. Huebner²⁴, F. Huegging²⁴, T.B. Huffman¹³³, M. Huhtinen³⁶, R. Hulsken⁵⁸, R.F.H. Hunter³⁴, N. Huseynov^{79,ab}, J. Huston¹⁰⁶, J. Huth⁵⁹, R. Hyneman¹⁵², S. Hyrych^{28a}, G. Iacobucci⁵⁴, G. Iakovidis²⁹, I. Ibragimov¹⁵⁰, L. Iconomidou-Fayard⁶⁴, P. Iengo³⁶, R. Ignazzi⁴⁰, R. Iguchi¹⁶², T. Iizawa⁵⁴, Y. Ikegami⁸¹, N. Ilic¹⁶⁵, H. Imam^{35a}, G. Introzzi^{70a,70b}, M. Iodice^{74a}, K. Iordanidou^{166a}, V. Ippolito^{72a,72b}, M. Ishino¹⁶², W. Islam¹²⁸, C. Issever^{19,46}, S. Istin^{12c}, J.M. Iturbe Ponce^{62a}, R. Iuppa^{75a,75b}, A. Ivina¹⁷⁸, J.M. Izen⁴³, V. Izzo^{69a}, P. Jacka¹³⁹, P. Jackson¹, R.M. Jacobs⁴⁶, B.P. Jaeger¹⁵¹, C.S. Jagfeld¹¹³, G. Jäkel¹⁸⁰, K.B. Jakobi⁹⁹, K. Jakobs⁵², T. Jakoubek¹⁷⁸, J. Jamieson⁵⁷, K.W. Janas^{83a}, G. Jarlskog⁹⁶, A.E. Jaspán⁹⁰, N. Javadov^{79,ab}, T. Javůrek³⁶, M. Javurkova¹⁰², F. Jeanneau¹⁴³, L. Jeanty¹³⁰, J. Jejelava^{158a}, P. Jenni^{52,e}, S. Jézéquel⁵, J. Jia¹⁵⁴, Z. Jia^{15c}, Y. Jiang^{60a}, S. Jiggins⁵², F.A. Jimenez Morales³⁸, J. Jimenez Pena¹¹⁴, S. Jin^{15c}, A. Jinaru^{27b}, O. Jinnouchi¹⁶³, H. Jivan^{33f}, P. Johansson¹⁴⁸, K.A. Johns⁷, C.A. Johnson⁶⁵, E. Jones¹⁷⁶, R.W.L. Jones⁸⁹, T.J. Jones⁹⁰, J. Jovicevic³⁶, X. Ju¹⁸, J.J. Junggeburth¹¹⁴, A. Juste Rozas^{14,x}, A. Kaczmarska⁸⁴, M. Kado^{72a,72b}, H. Kagan¹²⁶, M. Kagan¹⁵², A. Kahn³⁹, C. Kahra⁹⁹, T. Kaji¹⁷⁷, E. Kajomovitz¹⁵⁹, C.W. Kalderon²⁹, A. Kaluza⁹⁹, A. Kamenshchikov¹²², M. Kaneda¹⁶², N.J. Kang¹⁴⁴, S. Kang⁷⁸, Y. Kano¹¹⁶, J. Kanzaki⁸¹, D. Kar^{33f}, K. Karava¹³³, M.J. Kareem^{166b}, I. Karkanas¹⁶¹, S.N. Karpov⁷⁹, Z.M. Karpova⁷⁹, V. Kartvelishvili⁸⁹, A.N. Karyukhin¹²², E. Kasimi¹⁶¹, C. Kato^{60d}, J. Katzy⁴⁶, K. Kawade¹⁴⁹, K. Kawagoe⁸⁷, T. Kawaguchi¹¹⁶, T. Kawamoto¹⁴³, G. Kawamura⁵³, E.F. Kay¹⁷⁴, F.I. Kaya¹⁶⁸, S. Kazakos¹⁴, V.F. Kazanin^{121b,121a}, Y. Ke¹⁵⁴, J.M. Keaveney^{33a}, R. Keeler¹⁷⁴, J.S. Keller³⁴, D. Kelsey¹⁵⁵, J.J. Kempster²¹, J. Kendrick²¹, K.E. Kennedy³⁹, O. Kepka¹³⁹, S. Kersten¹⁸⁰, B.P. Kerševan⁹¹, S. Ketabchi Haghghat¹⁶⁵, F. Khalil-Zada¹³, M. Khandoga¹³⁴, A. Khanov¹²⁸, A.G. Kharlamov^{121b,121a}, T. Kharlamova^{121b,121a}, E.E. Khoda¹⁷³, T.J. Khoo¹⁹, G. Khoriauli¹⁷⁵, E. Khramov⁷⁹, J. Khubua^{158b}, S. Kido⁸², M. Kiehn³⁶, A. Kilgallon¹³⁰, E. Kim¹⁶³, Y.K. Kim³⁷, N. Kimura⁹⁴, A. Kirchhoff⁵³, D. Kirchmeier⁴⁸, J. Kirk¹⁴², A.E. Kiryunin¹¹⁴, T. Kishimoto¹⁶², D.P. Kisliuk¹⁶⁵, V. Kitali⁴⁶, C. Kitsaki¹⁰, O. Kivernyk²⁴, T. Klapdor-Kleingrothaus⁵², M. Klassen^{61a}, C. Klein³⁴, L. Klein¹⁷⁵, M.H. Klein¹⁰⁵, M. Klein⁹⁰, U. Klein⁹⁰, P. Klimek³⁶, A. Klimentov²⁹, F. Klimpel³⁶, T. Klingl²⁴, T. Klioutchnikova³⁶, F.F. Klitzner¹¹³, P. Kluit¹¹⁹, S. Kluth¹¹⁴, E. Kneringer⁷⁶, T.M. Knight¹⁶⁵, A. Knue⁵², D. Kobayashi⁸⁷, M. Kobel⁴⁸, M. Kocian¹⁵², T. Kodama¹⁶², P. Kodys¹⁴¹, D.M. Koeck¹⁵⁵, P.T. Koellig²⁴, T. Koffas³⁴, N.M. Köhler³⁶, M. Kolb¹⁴³, I. Koletsou⁵, T. Komarek¹²⁹, K. Köneke⁵², A.X.Y. Kong¹, T. Kono¹²⁵, V. Konstantinides⁹⁴, N. Konstantinidis⁹⁴, B. Konya⁹⁶, R. Kopeliansky⁶⁵, S. Koperny^{83a}, K. Korcyl⁸⁴, K. Kordas¹⁶¹, G. Koren¹⁶⁰, A. Korn⁹⁴, S. Korn⁵³, I. Korolkov¹⁴, E.V. Korolkova¹⁴⁸, N. Korotkova¹¹², O. Kortner¹¹⁴, S. Kortner¹¹⁴, V.V. Kostyukhin^{148,164}, A. Kotsokechagia⁶⁴, A. Kotwal⁴⁹, A. Koulouris⁹, A. Kourkoumeli-Charalampidi^{70a,70b}, C. Kourkoumelis⁹, E. Kourlitis⁶, R. Kowalewski¹⁷⁴, W. Kozanecki¹⁴³, A.S. Kozhin¹²², V.A. Kramarenko¹¹², G. Kramberger⁹¹, D. Krasnopevtsev^{60a}, M.W. Krasny¹³⁴, A. Krasznahorkay³⁶, J.A. Kremer⁹⁹, J. Kretzschmar⁹⁰, K. Kreul¹⁹, P. Krieger¹⁶⁵, F. Krieter¹¹³, S. Krishnamurthy¹⁰², A. Krishnan^{61b}, M. Krivos¹⁴¹, K. Krizka¹⁸, K. Kroeninger⁴⁷, H. Kroha¹¹⁴, J. Kroll¹³⁹, J. Kroll¹³⁵, K.S. Krowpman¹⁰⁶, U. Kruchonak⁷⁹, H. Krüger²⁴, N. Krumnack⁷⁸, M.C. Kruse⁴⁹, J.A. Krzysiak⁸⁴, A. Kubota¹⁶³, O. Kuchinskaia¹⁶⁴, S. Kудay^{4b}, D. Kuechler⁴⁶, J.T. Kuechler⁴⁶, S. Kuehn³⁶, T. Kuhl⁴⁶, V. Kukhtin⁷⁹, Y. Kulchitsky^{107,ae}, S. Kuleshov^{145b}, M. Kumar^{33f}, N. Kumari¹⁰¹, M. Kuna⁵⁸, A. Kupco¹³⁹, T. Kupfer⁴⁷, O. Kuprash⁵², H. Kurashige⁸², L.L. Kurchaninov^{166a}, Y.A. Kurochkin¹⁰⁷, A. Kurova¹¹¹, M.G. Kurth^{15a,15d}, E.S. Kuwertz³⁶, M. Kuze¹⁶³, A.K. Kvam¹⁴⁷, J. Kvita¹²⁹, T. Kwan¹⁰³, C. Lacasta¹⁷², F. Lacava^{72a,72b}, D.P.J. Lack¹⁰⁰, H. Lacker¹⁹, D. Lacour¹³⁴, E. Ladygin⁷⁹, R. Lafaye⁵, B. Laforge¹³⁴, T. Lagouri^{145c}, S. Lai⁵³, I.K. Lakomic^{83a}, N. Lalloue⁵⁸, J.E. Lambert¹²⁷, S. Lammers⁶⁵, W. Lampl⁷, C. Lampoudis¹⁶¹, E. Lançon²⁹, U. Landgraf⁵², M.P.J. Landon⁹², V.S. Lang⁵², J.C. Lange⁵³, R.J. Langenberg¹⁰², A.J. Lankford¹⁶⁹, F. Lanni²⁹, K. Lantzsch²⁴, A. Lanza^{70a}, A. Lapertosa^{55b,55a}, J.F. Laporte¹⁴³, T. Lari^{68a}, F. Lasagni Manghi^{23b,23a}, M. Lassnig³⁶, V. Latonova¹³⁹, T.S. Lau^{62a}, A. Laudrain⁹⁹, A. Laurier³⁴, M. Lavorgna^{69a,69b}, S.D. Lawlor⁹³, M. Lazzaroni^{68a,68b}, B. Le¹⁰⁰, A. Lebedev⁷⁸, M. LeBlanc⁷, T. LeCompte⁶, F. Ledroit-Guillon⁵⁸, A.C.A. Lee⁹⁴, C.A. Lee²⁹, G.R. Lee¹⁷, L. Lee⁵⁹, S.C. Lee¹⁵⁷, S. Lee⁷⁸, L.L. Leeuw^{33c}, B. Lefebvre^{166a}, H.P. Lefebvre⁹³, M. Lefebvre¹⁷⁴, C. Leggett¹⁸, K. Lehmann¹⁵¹, N. Lehmann²⁰, G. Lehmann Miotto³⁶, W.A. Leight⁴⁶, A. Leisos^{161,w}, M.A.L. Leite^{80c}, C.E. Leitgeb¹¹³, R. Leitner¹⁴¹, K.J.C. Leney⁴², T. Lenz²⁴, S. Leone^{71a}, C. Leonidopoulos⁵⁰, A. Leopold¹³⁴, C. Leroy¹⁰⁹, R. Les¹⁰⁶, C.G. Lester³², M. Levchenko¹³⁶, J. Levêque⁵, D. Levin¹⁰⁵, L.J. Levinson¹⁷⁸, D.J. Lewis²¹, B. Li^{15b}, B. Li¹⁰⁵, C-Q. Li^{60c,60d}, F. Li^{60c}, H. Li^{60a}, H. Li^{60b}, J. Li^{60c}, K. Li¹⁴⁷, L. Li^{60c}, M. Li^{15a,15d}, Q.Y. Li^{60a}, S. Li^{60d,60c,c}, X. Li⁴⁶, Y. Li⁴⁶, Z. Li^{60b}, Z. Li¹³³

Z. Li ¹⁰³, Z. Li ⁹⁰, Z. Liang ^{15a}, M. Liberatore ⁴⁶, B. Liberti ^{73a}, K. Lie ^{62c}, C.Y. Lin ³², K. Lin ¹⁰⁶, R.A. Linck ⁶⁵, R.E. Lindley ⁷, J.H. Lindon ²¹, A. Linss ⁴⁶, A.L. Lioni ⁵⁴, E. Lipeles ¹³⁵, A. Lipniacka ¹⁷, T.M. Liss ^{171,aj}, A. Lister ¹⁷³, J.D. Little ⁸, B. Liu ^{15a}, B.X. Liu ¹⁵¹, J.B. Liu ^{60a}, J.K.K. Liu ³⁷, K. Liu ^{60d,60c}, M. Liu ^{60a}, M.Y. Liu ^{60a}, P. Liu ^{15a}, X. Liu ^{60a}, Y. Liu ⁴⁶, Y. Liu ^{15a,15d}, Y.L. Liu ¹⁰⁵, Y.W. Liu ^{60a}, M. Livan ^{70a,70b}, A. Lleres ⁵⁸, J. Llorente Merino ¹⁵¹, S.L. Lloyd ⁹², E.M. Lobodzinska ⁴⁶, P. Loch ⁷, S. Loffredo ^{73a,73b}, T. Lohse ¹⁹, K. Lohwasser ¹⁴⁸, M. Lokajicek ¹³⁹, J.D. Long ¹⁷¹, R.E. Long ⁸⁹, I. Longarini ^{72a,72b}, L. Longo ³⁶, R. Longo ¹⁷¹, I. Lopez Paz ¹⁴, A. Lopez Solis ⁴⁶, J. Lorenz ¹¹³, N. Lorenzo Martinez ⁵, A.M. Lory ¹¹³, A. Lösle ⁵², X. Lou ^{45a,45b}, X. Lou ^{15a}, A. Lounis ⁶⁴, J. Love ⁶, P.A. Love ⁸⁹, J.J. Lozano Bahilo ¹⁷², G. Lu ^{15a}, M. Lu ^{60a}, S. Lu ¹³⁵, Y.J. Lu ⁶³, H.J. Lubatti ¹⁴⁷, C. Luci ^{72a,72b}, F.L. Lucio Alves ^{15c}, A. Lucotte ⁵⁸, F. Luehring ⁶⁵, I. Luise ¹⁵⁴, L. Luminari ^{72a}, B. Lund-Jensen ¹⁵³, N.A. Luongo ¹³⁰, M.S. Lutz ¹⁶⁰, D. Lynn ²⁹, H. Lyons ⁹⁰, R. Lysak ¹³⁹, E. Lytken ⁹⁶, F. Lyu ^{15a}, V. Lyubushkin ⁷⁹, T. Lyubushkina ⁷⁹, H. Ma ²⁹, L.L. Ma ^{60b}, Y. Ma ⁹⁴, D.M. Mac Donell ¹⁷⁴, G. Maccarrone ⁵¹, C.M. Macdonald ¹⁴⁸, J.C. MacDonald ¹⁴⁸, R. Madar ³⁸, W.F. Mader ⁴⁸, M. Madugoda Ralalage Don ¹²⁸, N. Madysa ⁴⁸, J. Maeda ⁸², T. Maeno ²⁹, M. Maerker ⁴⁸, V. Magerl ⁵², J. Magro ^{66a,66c}, D.J. Mahon ³⁹, C. Maidantchik ^{80b}, A. Maio ^{138a,138b,138d}, K. Maj ^{83a}, O. Majersky ^{28a}, S. Majewski ¹³⁰, N. Makovec ⁶⁴, B. Malaescu ¹³⁴, Pa. Malecki ⁸⁴, V.P. Maleev ¹³⁶, F. Malek ⁵⁸, D. Malito ^{41b,41a}, U. Mallik ⁷⁷, C. Malone ³², S. Maltezos ¹⁰, S. Malyukov ⁷⁹, J. Mamuzic ¹⁷², G. Mancini ⁵¹, J.P. Mandalia ⁹², I. Mandić ⁹¹, L. Manhaes de Andrade Filho ^{80a}, I.M. Maniatis ¹⁶¹, M. Manisha ¹⁴³, J. Manjarres Ramos ⁴⁸, K.H. Mankinen ⁹⁶, A. Mann ¹¹³, A. Manousos ⁷⁶, B. Mansoulie ¹⁴³, I. Manthos ¹⁶¹, S. Manzoni ¹¹⁹, A. Marantis ¹⁶¹, L. Marchese ¹³³, G. Marchiori ¹³⁴, M. Marcisovsky ¹³⁹, L. Marcoccia ^{73a,73b}, C. Marcon ⁹⁶, M. Marjanovic ¹²⁷, Z. Marshall ¹⁸, S. Marti-Garcia ¹⁷², T.A. Martin ¹⁷⁶, V.J. Martin ⁵⁰, B. Martin dit Latour ¹⁷, L. Martinelli ^{74a,74b}, M. Martinez ^{14,x}, P. Martinez Agullo ¹⁷², V.I. Martinez Outschoorn ¹⁰², S. Martin-Haugh ¹⁴², V.S. Martoiu ^{27b}, A.C. Martyniuk ⁹⁴, A. Marzin ³⁶, S.R. Maschek ¹¹⁴, L. Masetti ⁹⁹, T. Mashimo ¹⁶², R. Mashinistov ¹¹⁰, J. Masik ¹⁰⁰, A.L. Maslennikov ^{121b,121a}, L. Massa ^{23b,23a}, P. Massarotti ^{69a,69b}, P. Mastrandrea ^{71a,71b}, A. Mastroberardino ^{41b,41a}, T. Masubuchi ¹⁶², D. Matakias ²⁹, T. Mathisen ¹⁷⁰, A. Matic ¹¹³, N. Matsuzawa ¹⁶², J. Maurer ^{27b}, B. Maček ⁹¹, D.A. Maximov ^{121b,121a}, R. Mazini ¹⁵⁷, I. Maznas ¹⁶¹, S.M. Mazza ¹⁴⁴, C. Mc Ginn ²⁹, J.P. Mc Gowan ¹⁰³, S.P. Mc Kee ¹⁰⁵, T.G. McCarthy ¹¹⁴, W.P. McCormack ¹⁸, E.F. McDonald ¹⁰⁴, A.E. McDougall ¹¹⁹, J.A. Mcfayden ¹⁵⁵, G. Mchedlidze ^{158b}, M.A. McKay ⁴², K.D. McLean ¹⁷⁴, S.J. McMahon ¹⁴², P.C. McNamara ¹⁰⁴, R.A. McPherson ^{174,aa}, J.E. Mdhului ^{33f}, Z.A. Meadows ¹⁰², S. Meehan ³⁶, T. Megy ³⁸, S. Mehlhase ¹¹³, A. Mehta ⁹⁰, B. Meirose ⁴³, D. Melini ¹⁵⁹, B.R. Mellado Garcia ^{33f}, F. Meloni ⁴⁶, A. Melzer ²⁴, E.D. Mendes Gouveia ^{138a,138e}, A.M. Mendes Jacques Da Costa ²¹, H.Y. Meng ¹⁶⁵, L. Meng ³⁶, S. Menke ¹¹⁴, E. Meoni ^{41b,41a}, S.A.M. Merkt ¹³⁷, C. Merlassino ¹³³, P. Mermoud ⁵⁴, L. Merola ^{69a,69b}, C. Meroni ^{68a}, G. Merz ¹⁰⁵, O. Meshkov ^{112,110}, J.K.R. Meshreki ¹⁵⁰, J. Metcalfe ⁶, A.S. Mete ⁶, C. Meyer ⁶⁵, J-P. Meyer ¹⁴³, M. Michetti ¹⁹, R.P. Middleton ¹⁴², L. Mijović ⁵⁰, G. Mikenberg ¹⁷⁸, M. Mikestikova ¹³⁹, M. Mikuž ⁹¹, H. Mildner ¹⁴⁸, A. Milic ¹⁶⁵, C.D. Milke ⁴², D.W. Miller ³⁷, L.S. Miller ³⁴, A. Milov ¹⁷⁸, D.A. Milstead ^{45a,45b}, A.A. Minaenko ¹²², I.A. Minashvili ^{158b}, L. Mince ⁵⁷, A.I. Mincer ¹²⁴, B. Mindur ^{83a}, M. Mineev ⁷⁹, Y. Minegishi ¹⁶², Y. Mino ⁸⁵, L.M. Mir ¹⁴, M. Miralles Lopez ¹⁷², M. Mironova ¹³³, T. Mitani ¹⁷⁷, V.A. Mitsou ¹⁷², M. Mittal ^{60c}, O. Miu ¹⁶⁵, P.S. Miyagawa ⁹², Y. Miyazaki ⁸⁷, A. Mizukami ⁸¹, J.U. Mjörnmark ⁹⁶, T. Mkrtchyan ^{61a}, M. Mlynarikova ¹²⁰, T. Moa ^{45a,45b}, S. Mobius ⁵³, K. Mochizuki ¹⁰⁹, P. Moder ⁴⁶, P. Mogg ¹¹³, S. Mohapatra ³⁹, G. Mokgatitswane ^{33f}, B. Mondal ¹⁵⁰, S. Mondal ¹⁴⁰, K. Mönig ⁴⁶, E. Monnier ¹⁰¹, A. Montalbano ¹⁵¹, J. Montejo Berlingen ³⁶, M. Montella ⁹⁴, F. Monticelli ⁸⁸, N. Morange ⁶⁴, A.L. Moreira De Carvalho ^{138a}, M. Moreno Llácer ¹⁷², C. Moreno Martinez ¹⁴, P. Morettini ^{55b}, M. Morgenstern ¹⁵⁹, S. Morgenstern ¹⁷⁶, D. Mori ¹⁵¹, M. Morii ⁵⁹, M. Morinaga ¹⁷⁷, V. Morisbak ¹³², A.K. Morley ³⁶, A.P. Morris ⁹⁴, L. Morvaj ³⁶, P. Moschovakos ³⁶, B. Moser ¹¹⁹, M. Mosidze ^{158b}, T. Moskalets ⁵², P. Moskvitina ¹¹⁸, J. Moss ^{31,o}, E.J.W. Moyse ¹⁰², S. Muanza ¹⁰¹, J. Mueller ¹³⁷, D. Muenstermann ⁸⁹, G.A. Mullier ⁹⁶, J.J. Mullin ¹³⁵, D.P. Mungo ^{68a,68b}, J.L. Munoz Martinez ¹⁴, F.J. Munoz Sanchez ¹⁰⁰, M. Murin ¹⁰⁰, P. Murin ^{28b}, W.J. Murray ^{176,142}, A. Murrone ^{68a,68b}, J.M. Muse ¹²⁷, M. Muškinja ¹⁸, C. Mwewa ²⁹, A.G. Myagkov ^{122,af}, A.A. Myers ¹³⁷, G. Myers ⁶⁵, J. Myers ¹³⁰, M. Myska ¹⁴⁰, B.P. Nachman ¹⁸, O. Nackenhorst ⁴⁷, A. Nag Nag ⁴⁸, K. Nagai ¹³³, K. Nagano ⁸¹, J.L. Nagle ²⁹, E. Nagy ¹⁰¹, A.M. Nairz ³⁶, Y. Nakahama ¹¹⁶, K. Nakamura ⁸¹, H. Nanjo ¹³¹, F. Napolitano ^{61a}, R.F. Naranjo Garcia ⁴⁶, R. Narayan ⁴², I. Naryshkin ¹³⁶, M. Naseri ³⁴, T. Naumann ⁴⁶, G. Navarro ^{22a}, J. Navarro-Gonzalez ¹⁷², P.Y. Nechaeva ¹¹⁰, F. Nechansky ⁴⁶, T.J. Neep ²¹, A. Negri ^{70a,70b}, M. Negrini ^{23b}, C. Nellist ¹¹⁸, C. Nelson ¹⁰³, K. Nelson ¹⁰⁵, M.E. Nelson ^{45a,45b}, S. Nemecek ¹³⁹, M. Nessi ^{36,g}, M.S. Neubauer ¹⁷¹, F. Neuhaus ⁹⁹,

M. Neumann¹⁸⁰, R. Newhouse¹⁷³, P.R. Newman²¹, C.W. Ng¹³⁷, Y.S. Ng¹⁹, Y.W.Y. Ng¹⁶⁹, B. Ngair^{35f}, H.D.N. Nguyen¹⁰¹, T. Nguyen Manh¹⁰⁹, E. Nibigira³⁸, R.B. Nickerson¹³³, R. Nicolaidou¹⁴³, D.S. Nielsen⁴⁰, J. Nielsen¹⁴⁴, M. Niemeyer⁵³, N. Nikiforou¹¹, V. Nikolaenko^{122.af}, I. Nikolic-Audit¹³⁴, K. Nikolopoulos²¹, P. Nilsson²⁹, H.R. Nindhito⁵⁴, A. Nisati^{72a}, N. Nishu³, R. Nisius¹¹⁴, T. Nitta¹⁷⁷, T. Nobe¹⁶², D.L. Noel³², Y. Noguchi⁸⁵, I. Nomidis¹³⁴, M.A. Nomura²⁹, M.B. Norfolk¹⁴⁸, R.R.B. Norisam⁹⁴, J. Novak⁹¹, T. Novak⁴⁶, O. Novgorodova⁴⁸, L. Novotny¹⁴⁰, R. Novotny¹¹⁷, L. Nozka¹²⁹, K. Ntekas¹⁶⁹, E. Nurse⁹⁴, F.G. Oakham^{34.ak}, J. Ocariz¹³⁴, A. Ochi⁸², I. Ochoa^{138a}, J.P. Ochoa-Ricoux^{145a}, K. O'Connor²⁶, S. Oda⁸⁷, S. Odaka⁸¹, S. Oerdek⁵³, A. Ogrodnik^{83a}, A. Oh¹⁰⁰, C.C. Ohm¹⁵³, H. Oide¹⁶³, R. Oishi¹⁶², M.L. Ojeda¹⁶⁵, Y. Okazaki⁸⁵, M.W. O'Keefe⁹⁰, Y. Okumura¹⁶², A. Olariu^{27b}, L.F. Oleiro Seabra^{138a}, S.A. Olivares Pino^{145c}, D. Oliveira Damazio²⁹, D. Oliveira Goncalves^{80a}, J.L. Oliver¹, M.J.R. Olsson¹⁶⁹, A. Olszewski⁸⁴, J. Olszowska⁸⁴, Ö.O. Öncel²⁴, D.C. O'Neil¹⁵¹, A.P. O'Neill¹³³, A. Onofre^{138a,138e}, P.U.E. Onyisi¹¹, H. Oppen¹³², R.G. Oreamuno Madriz¹²⁰, M.J. Oreglia³⁷, G.E. Orellana⁸⁸, D. Orestano^{74a,74b}, N. Orlando¹⁴, R.S. Orr¹⁶⁵, V. O'Shea⁵⁷, R. Ospanov^{60a}, G. Otero y Garzon³⁰, H. Otono⁸⁷, P.S. Ott^{61a}, G.J. Ottino¹⁸, M. Ouchrif^{35e}, J. Ouellette²⁹, F. Ould-Saada¹³², A. Ouraou^{143.*}, Q. Ouyang^{15a}, M. Owen⁵⁷, R.E. Owen¹⁴², V.E. Ozcan^{12c}, N. Ozturk⁸, J. Pacalt¹²⁹, H.A. Pacey³², K. Pachal⁴⁹, A. Pacheco Pages¹⁴, C. Padilla Aranda¹⁴, S. Pagan Griso¹⁸, G. Palacino⁶⁵, S. Palazzo⁵⁰, S. Palestini³⁶, M. Palka^{83b}, P. Palni^{83a}, D.K. Panchal¹¹, C.E. Pandini⁵⁴, J.G. Panduro Vazquez⁹³, P. Pani⁴⁶, G. Panizzo^{66a,66c}, L. Paolozzi⁵⁴, C. Papadatos¹⁰⁹, S. Parajuli⁴², A. Paramonov⁶, C. Paraskevopoulos¹⁰, D. Paredes Hernandez^{62b}, S.R. Paredes Saenz¹³³, B. Parida¹⁷⁸, T.H. Park¹⁶⁵, A.J. Parker³¹, M.A. Parker³², F. Parodi^{55b,55a}, E.W. Parrish¹²⁰, J.A. Parsons³⁹, U. Parzefall⁵², L. Pascual Dominguez¹³⁴, V.R. Pascuzzi¹⁸, J.M.P. Pasner¹⁴⁴, F. Pasquali¹¹⁹, E. Pasqualucci^{72a}, S. Passaggio^{55b}, F. Pastore⁹³, P. Pasuwan^{45a,45b}, J.R. Pater¹⁰⁰, A. Pathak^{179,k}, J. Patton⁹⁰, T. Pauly³⁶, J. Parkes¹⁵², M. Pedersen¹³², L. Pedraza Diaz¹¹⁸, R. Pedro^{138a}, T. Peiffer⁵³, S.V. Peleganchuk^{121b,121a}, O. Penc¹³⁹, C. Peng^{62b}, H. Peng^{60a}, M. Penzin¹⁶⁴, B.S. Peralva^{80a}, M.M. Perego⁶⁴, A.P. Pereira Peixoto^{138a}, L. Pereira Sanchez^{45a,45b}, D.V. Perepelitsa²⁹, E. Perez Codina^{166a}, M. Perganti¹⁰, L. Perini^{68a,68b}, H. Pernegger³⁶, S. Perrella³⁶, A. Perrevoort¹¹⁹, K. Peters⁴⁶, R.F.Y. Peters¹⁰⁰, B.A. Petersen³⁶, T.C. Petersen⁴⁰, E. Petit¹⁰¹, V. Petousis¹⁴⁰, C. Petridou¹⁶¹, P. Petroff⁶⁴, F. Petrucci^{74a,74b}, M. Pettee¹⁸¹, N.E. Pettersson¹⁰², K. Petukhova¹⁴¹, A. Peyaud¹⁴³, R. Pezoa^{145d}, L. Pezzotti^{70a,70b}, G. Pezzullo¹⁸¹, T. Pham¹⁰⁴, P.W. Phillips¹⁴², M.W. Phipps¹⁷¹, G. Piacquadio¹⁵⁴, E. Pianori¹⁸, F. Piazza^{68a,68b}, A. Picazio¹⁰², R. Piegai³⁰, D. Pietreanu^{27b}, J.E. Pilcher³⁷, A.D. Pilkington¹⁰⁰, M. Pinamonti^{66a,66c}, J.L. Pinfold³, C. Pitman Donaldson⁹⁴, D.A. Pizzi³⁴, L. Pizzimento^{73a,73b}, A. Pizzini¹¹⁹, M.-A. Pleier²⁹, V. Plesanovs⁵², V. Pleskot¹⁴¹, E. Plotnikova⁷⁹, P. Podberezko^{121b,121a}, R. Poettgen⁹⁶, R. Poggi⁵⁴, L. Poggioli¹³⁴, I. Pogrebnyak¹⁰⁶, D. Pohl²⁴, I. Pokharel⁵³, G. Polesello^{70a}, A. Poley^{151,166a}, A. Policicchio^{72a,72b}, R. Polifka¹⁴¹, A. Polini^{23b}, C.S. Pollard⁴⁶, Z.B. Pollock¹²⁶, V. Polychronakos²⁹, D. Ponomarenko¹¹¹, L. Pontecorvo³⁶, S. Popa^{27a}, G.A. Popeneciu^{27d}, L. Portales⁵, D.M. Portillo Quintero⁵⁸, S. Pospisil¹⁴⁰, P. Postolache^{27c}, K. Potamianos¹³³, I.N. Potrap⁷⁹, C.J. Potter³², H. Potti¹¹, T. Poulsen⁴⁶, J. Poveda¹⁷², T.D. Powell¹⁴⁸, G. Pownall⁴⁶, M.E. Pozo Astigarraga³⁶, A. Prades Ibanez¹⁷², P. Pralavorio¹⁰¹, M.M. Prapa⁴⁴, S. Prell⁷⁸, D. Price¹⁰⁰, M. Primavera^{67a}, M.A. Principe Martin⁹⁸, M.L. Proffitt¹⁴⁷, N. Proklova¹¹¹, K. Prokofiev^{62c}, F. Prokoshin⁷⁹, S. Protopopescu²⁹, J. Proudfoot⁶, M. Przybycien^{83a}, D. Pudzha¹³⁶, P. Puzo⁶⁴, D. Pyatiizbyantseva¹¹¹, J. Qian¹⁰⁵, Y. Qin¹⁰⁰, A. Quadt⁵³, M. Queitsch-Maitland³⁶, G. Rabanal Bolanos⁵⁹, F. Ragusa^{68a,68b}, G. Rahal⁹⁷, J.A. Raine⁵⁴, S. Rajagopalan²⁹, K. Ran^{15a,15d}, D.F. Rassloff^{61a}, D.M. Rauch⁴⁶, S. Rave⁹⁹, B. Ravina⁵⁷, I. Ravinovich¹⁷⁸, M. Raymond³⁶, A.L. Read¹³², N.P. Readioff¹⁴⁸, M. Reale^{67a,67b}, D.M. Rebuffi^{70a,70b}, G. Redlinger²⁹, K. Reeves⁴³, D. Reikher¹⁶⁰, A. Reiss⁹⁹, A. Rej¹⁵⁰, C. Rembser³⁶, A. Renardi⁴⁶, M. Renda^{27b}, M.B. Rendel¹¹⁴, A.G. Rennie⁵⁷, S. Resconi^{68a}, E.D. Resseguie¹⁸, S. Rettie⁹⁴, B. Reynolds¹²⁶, E. Reynolds²¹, M. Rezaei Estabragh¹⁸⁰, O.L. Rezanova^{121b,121a}, P. Reznicek¹⁴¹, E. Ricci^{75a,75b}, R. Richter¹¹⁴, S. Richter⁴⁶, E. Richter-Was^{83b}, M. Ridel¹³⁴, P. Rieck¹¹⁴, O. Rifki⁴⁶, M. Rijssenbeek¹⁵⁴, A. Rimoldi^{70a,70b}, M. Rimoldi⁴⁶, L. Rinaldi^{23b}, T.T. Rinn¹⁷¹, M.P. Rinnagel¹¹³, G. Ripellino¹⁵³, I. Riu¹⁴, P. Rivadeneira⁴⁶, J.C. Rivera Vergara¹⁷⁴, F. Rizatdinova¹²⁸, E. Rizvi⁹², C. Rizzi⁵⁴, S.H. Robertson^{103.aa}, M. Robin⁴⁶, D. Robinson³², C.M. Robles Gajardo^{145d}, M. Robles Manzano⁹⁹, A. Robson⁵⁷, A. Rocchi^{73a,73b}, C. Roda^{71a,71b}, S. Rodriguez Bosca¹⁷², A. Rodriguez Rodriguez⁵², A.M. Rodriguez Vera^{166b}, S. Roe³⁶, J. Roggel¹⁸⁰, O. Røhne¹³², R.A. Rojas^{145d}, B. Roland⁵², C.P.A. Roland⁶⁵, J. Roloff²⁹, A. Romaniouk¹¹¹, M. Romano^{23b,23a}, N. Rompotis⁹⁰, M. Ronzani¹²⁴, L. Roos¹³⁴, S. Rosati^{72a}, G. Rosin¹⁰², B.J. Rosser¹³⁵, E. Rossi¹⁶⁵, E. Rossi⁵, E. Rossi^{69a,69b}, L.P. Rossi^{55b},

L. Rossini⁴⁶, R. Rosten¹²⁶, M. Rotaru^{27b}, B. Rottler⁵², D. Rousseau⁶⁴, D. Rousso³², G. Rovelli^{70a,70b}, A. Roy¹¹, A. Rozanov¹⁰¹, Y. Rozen¹⁵⁹, X. Ruan^{33f}, A.J. Ruby⁹⁰, T.A. Ruggeri¹, F. Rühr⁵², A. Ruiz-Martinez¹⁷², A. Rummler³⁶, Z. Rurikova⁵², N.A. Rusakovich⁷⁹, H.L. Russell³⁶, L. Rustige³⁸, J.P. Rutherford⁷, E.M. Rüttinger¹⁴⁸, M. Rybar¹⁴¹, E.B. Rye¹³², A. Ryzhov¹²², J.A. Sabater Iglesias⁴⁶, P. Sabatini¹⁷², L. Sabetta^{72a,72b}, H.F.-W. Sadrozinski¹⁴⁴, R. Sadykov⁷⁹, F. Safai Tehrani^{72a}, B. Safarzadeh Samani¹⁵⁵, M. Safdari¹⁵², P. Saha¹²⁰, S. Saha¹⁰³, M. Sahinsoy¹¹⁴, A. Sahu¹⁸⁰, M. Saimpert³⁶, M. Saito¹⁶², T. Saito¹⁶², D. Salamani⁵⁴, G. Salamanna^{74a,74b}, A. Salnikov¹⁵², J. Salt¹⁷², A. Salvador Salas¹⁴, D. Salvatore^{41b,41a}, F. Salvatore¹⁵⁵, A. Salzburger³⁶, D. Sammel⁵², D. Sampsonidis¹⁶¹, D. Sampsonidou^{60d,60c}, J. Sánchez¹⁷², A. Sanchez Pineda^{66a,36,66c}, H. Sandaker¹³², C.O. Sander⁴⁶, I.G. Sanderswood⁸⁹, M. Sandhoff¹⁸⁰, C. Sandoval^{22b}, D.P.C. Sankey¹⁴², M. Sannino^{55b,55a}, Y. Sano¹¹⁶, A. Sansoni⁵¹, C. Santoni³⁸, H. Santos^{138a,138b}, S.N. Santpur¹⁸, A. Santra¹⁷⁸, K.A. Saoucha¹⁴⁸, A. Sapronov⁷⁹, J.G. Saraiva^{138a,138d}, O. Sasaki⁸¹, K. Sato¹⁶⁷, C. Sauer^{61b}, F. Sauerburger⁵², E. Sauvan⁵, P. Savard^{165,ak}, R. Sawada¹⁶², C. Sawyer¹⁴², L. Sawyer⁹⁵, I. Sayago Galvan¹⁷², C. Sbarra^{23b}, A. Sbrizzi^{66a,66c}, T. Scanlon⁹⁴, J. Schaarschmidt¹⁴⁷, P. Schacht¹¹⁴, D. Schaefer³⁷, L. Schaefer¹³⁵, U. Schäfer⁹⁹, A.C. Schaffer⁶⁴, D. Schaile¹¹³, R.D. Schamberger¹⁵⁴, E. Schanet¹¹³, C. Scharf¹⁹, N. Scharmberg¹⁰⁰, V.A. Schegelsky¹³⁶, D. Scheirich¹⁴¹, F. Schenck¹⁹, M. Schernau¹⁶⁹, C. Schiavi^{55b,55a}, L.K. Schildgen²⁴, Z.M. Schillaci²⁶, E.J. Schioppa^{67a,67b}, M. Schioppa^{41b,41a}, B. Schlag⁹⁹, K.E. Schleicher⁵², S. Schlenker³⁶, K. Schmieden⁹⁹, C. Schmitt⁹⁹, S. Schmitt⁴⁶, L. Schoeffel¹⁴³, A. Schoening^{61b}, P.G. Scholer⁵², E. Schopf¹³³, M. Schott⁹⁹, J. Schovancova³⁶, S. Schramm⁵⁴, F. Schroeder¹⁸⁰, A. Schulte⁹⁹, H.-C. Schultz-Coulon^{61a}, M. Schumacher⁵², B.A. Schumm¹⁴⁴, Ph. Schune¹⁴³, A. Schwartzman¹⁵², T.A. Schwarz¹⁰⁵, Ph. Schwemling¹⁴³, R. Schwienhorst¹⁰⁶, A. Sciandra¹⁴⁴, G. Sciolla²⁶, F. Scuri^{71a}, F. Scutti¹⁰⁴, C.D. Sebastiani⁹⁰, K. Sedlaczek⁴⁷, P. Seema¹⁹, S.C. Seidel¹¹⁷, A. Seiden¹⁴⁴, B.D. Seidlitz²⁹, T. Seiss³⁷, C. Seitz⁴⁶, J.M. Seixas^{80b}, G. Sekhniaidze^{69a}, S.J. Sekula⁴², L.P. Selem⁵, N. Semprini-Cesari^{23b,23a}, S. Sen⁴⁹, C. Serfon²⁹, L. Serin⁶⁴, L. Serkin^{66a,66b}, M. Sessa^{60a}, H. Severini¹²⁷, S. Sevova¹⁵², F. Sforza^{55b,55a}, A. Sfyrla⁵⁴, E. Shabalina⁵³, J.D. Shahinian¹³⁵, N.W. Shaikh^{45a,45b}, D. Shaked Renous¹⁷⁸, L.Y. Shan^{15a}, M. Shapiro¹⁸, A. Sharma³⁶, A.S. Sharma¹, S. Sharma⁴⁶, P.B. Shatalov¹²³, K. Shaw¹⁵⁵, S.M. Shaw¹⁰⁰, M. Shehade¹⁷⁸, Y. Shen¹²⁷, P. Sherwood⁹⁴, L. Shi⁹⁴, C.O. Shimmin¹⁸¹, Y. Shimogama¹⁷⁷, M. Shimojima¹¹⁵, J.D. Shinner⁹³, I.P.J. Shipsey¹³³, S. Shirabe¹⁶³, M. Shiyakova⁷⁹, J. Shlomi¹⁷⁸, M.J. Shochet³⁷, J. Shojaii¹⁰⁴, D.R. Shope¹⁵³, S. Shrestha¹²⁶, E.M. Shrif^{33f}, M.J. Shroff¹⁷⁴, E. Shulga¹⁷⁸, P. Sicho¹³⁹, A.M. Sickles¹⁷¹, E. Sideras Haddad^{33f}, O. Sidiropoulou³⁶, A. Sidoti^{23b,23a}, F. Siegert⁴⁸, Dj. Sijacki¹⁶, M.V. Silva Oliveira³⁶, S.B. Silverstein^{45a}, S. Simion⁶⁴, R. Simoniello³⁶, S. Simsek^{12b}, P. Sinervo¹⁶⁵, V. Sinetckii¹¹², S. Singh¹⁵¹, S. Sinha^{33f}, M. Sioli^{23b,23a}, I. Siral¹³⁰, S.Yu. Sivoklov¹¹², J. Sjölin^{45a,45b}, A. Skaf⁵³, E. Skorda⁹⁶, P. Skubic¹²⁷, M. Slawinska⁸⁴, K. Sliwa¹⁶⁸, V. Smakhtin¹⁷⁸, B.H. Smart¹⁴², J. Smiesko¹⁴¹, S.Yu. Smirnov¹¹¹, Y. Smirnov¹¹¹, L.N. Smirnova^{112,s}, O. Smirnova⁹⁶, E.A. Smith³⁷, H.A. Smith¹³³, M. Smizanska⁸⁹, K. Smolek¹⁴⁰, A. Smykiewicz⁸⁴, A.A. Snesarev¹¹⁰, H.L. Snoek¹¹⁹, I.M. Snyder¹³⁰, S. Snyder²⁹, R. Sobie^{174,aa}, A. Soffer¹⁶⁰, A. Søgaard⁵⁰, F. Sohns⁵³, C.A. Solans Sanchez³⁶, E.Yu. Soldatov¹¹¹, U. Soldevila¹⁷², A.A. Solodkov¹²², S. Solomon⁵², A. Soloshenko⁷⁹, O.V. Solovyanov¹²², V. Solovyev¹³⁶, P. Sommer¹⁴⁸, H. Son¹⁶⁸, A. Sonay¹⁴, W.Y. Song^{166b}, A. Sopczak¹⁴⁰, A.L. Sapiro⁹⁴, F. Sopkova^{28b}, S. Sottocornola^{70a,70b}, R. Soualah^{66a,66c}, A.M. Soukharev^{121b,121a}, Z. Soumami^{35f}, D. South⁴⁶, S. Spagnolo^{67a,67b}, M. Spalla¹¹⁴, M. Spangenberg¹⁷⁶, F. Spanò⁹³, D. Sperlich⁵², T.M. Spieker^{61a}, G. Spigo³⁶, M. Spina¹⁵⁵, D.P. Spiteri⁵⁷, M. Spousta¹⁴¹, A. Stabile^{68a,68b}, B.L. Stamas¹²⁰, R. Stamen^{61a}, M. Stamenkovic¹¹⁹, A. Stampekis²¹, E. Stanecka⁸⁴, B. Stanislaus¹³³, M.M. Stanitzki⁴⁶, M. Stankaityte¹³³, B. Stapf⁴⁶, E.A. Starchenko¹²², G.H. Stark¹⁴⁴, J. Stark¹⁰¹, D.M. Starko^{166b}, P. Staroba¹³⁹, P. Starovoitov^{61a}, S. Stärz¹⁰³, R. Staszewski⁸⁴, G. Stavropoulos⁴⁴, P. Steinberg²⁹, A.L. Steinhebel¹³⁰, B. Stelzer^{151,166a}, H.J. Stelzer¹³⁷, O. Stelzer-Chilton^{166a}, H. Stenzel⁵⁶, T.J. Stevenson¹⁵⁵, G.A. Stewart³⁶, M.C. Stockton³⁶, G. Stoica^{27b}, M. Stolarski^{138a}, S. Stonjek¹¹⁴, A. Straessner⁴⁸, J. Strandberg¹⁵³, S. Strandberg^{45a,45b}, M. Strauss¹²⁷, T. Strebler¹⁰¹, P. Strizenec^{28b}, R. Ströhmer¹⁷⁵, D.M. Strom¹³⁰, L.R. Strom⁴⁶, R. Stroynowski⁴², A. Strubig^{45a,45b}, S.A. Stucci²⁹, B. Stugu¹⁷, J. Stupak¹²⁷, N.A. Styles⁴⁶, D. Su¹⁵², S. Su^{60a}, W. Su^{60d,147,60c}, X. Su^{60a}, N.B. Suarez¹³⁷, K. Sugizaki¹⁶², V.V. Sulin¹¹⁰, M.J. Sullivan⁹⁰, D.M.S. Sultan⁵⁴, S. Sultansoy^{4c}, T. Sumida⁸⁵, S. Sun¹⁰⁵, S. Sun¹⁷⁹, X. Sun¹⁰⁰, C.J.E. Suster¹⁵⁶, M.R. Sutton¹⁵⁵, M. Svatos¹³⁹, M. Swiatlowski^{166a}, S.P. Swift², T. Swirski¹⁷⁵, A. Sydorenko⁹⁹, I. Sykora^{28a}, M. Sykora¹⁴¹, T. Sykora¹⁴¹, D. Ta⁹⁹, K. Tackmann^{46,y}, A. Taffard¹⁶⁹, R. Tafirout^{166a}, E. Tagiev¹²², R.H.M. Taibah¹³⁴,

R. Takashima⁸⁶, K. Takeda⁸², T. Takeshita¹⁴⁹, E.P. Takeva⁵⁰, Y. Takubo⁸¹, M. Talby¹⁰¹,
A.A. Talyshev^{121b,121a}, K.C. Tam^{62b}, N.M. Tamir¹⁶⁰, J. Tanaka¹⁶², R. Tanaka⁶⁴, S. Tapia Araya¹⁷¹,
S. Tapprogge⁹⁹, A. Tarek Abouelfadl Mohamed¹⁰⁶, S. Tarem¹⁵⁹, K. Tariq^{60b}, G. Tarna^{27b,f},
G.F. Tartarelli^{68a}, P. Tas¹⁴¹, M. Tasevsky¹³⁹, E. Tassi^{41b,41a}, G. Tateno¹⁶², Y. Tayalati^{35f}, G.N. Taylor¹⁰⁴,
W. Taylor^{166b}, H. Teagle⁹⁰, A.S. Tee⁸⁹, R. Teixeira De Lima¹⁵², P. Teixeira-Dias⁹³, H. Ten Kate³⁶,
J.J. Teoh¹¹⁹, K. Terashi¹⁶², J. Terron⁹⁸, S. Terzo¹⁴, M. Testa⁵¹, R.J. Teuscher^{165,aa}, N. Themistokleous⁵⁰,
T. Theveneaux-Pelzer¹⁹, D.W. Thomas⁹³, J.P. Thomas²¹, E.A. Thompson⁴⁶, P.D. Thompson²¹,
E. Thomson¹³⁵, E.J. Thorpe⁹², Y. Tian⁵³, V.O. Tikhomirov^{110.ag}, Yu.A. Tikhonov^{121b,121a},
S. Timoshenko¹¹¹, P. Tipton¹⁸¹, S. Tisserant¹⁰¹, S.H. Tlou^{33f}, A. Tnourji³⁸, K. Todome^{23b,23a},
S. Todorova-Nova¹⁴¹, S. Todt⁴⁸, M. Togawa⁸¹, J. Tojo⁸⁷, S. Tokár^{28a}, K. Tokushuku⁸¹, E. Tolley¹²⁶,
R. Tombs³², M. Tomoto^{81,116}, L. Tompkins¹⁵², P. Tornambe¹⁰², E. Torrence¹³⁰, H. Torres⁴⁸,
E. Torr  Pastor¹⁷², M. Toscani³⁰, C. Tosciri³⁷, J. Toth^{101,z}, D.R. Tovey¹⁴⁸, A. Traet¹⁷, C.J. Treado¹²⁴,
T. Trefzger¹⁷⁵, A. Tricoli²⁹, I.M. Trigger^{166a}, S. Trincaz-Duvold¹³⁴, D.A. Trischuk¹⁷³, W. Trischuk¹⁶⁵,
B. Trocm ⁵⁸, A. Trofymov⁶⁴, C. Troncon^{68a}, F. Trovato¹⁵⁵, L. Truong^{33c}, M. Trzebinski⁸⁴, A. Trzupek⁸⁴,
F. Tsai¹⁵⁴, A. Tsiamis¹⁶¹, P.V. Tsiarehshka^{107,ae}, A. Tsirigotis^{161,w}, V. Tsiskaridze¹⁵⁴, E.G. Tskhadadze^{158a},
M. Tsopoulou¹⁶¹, I.I. Tsukerman¹²³, V. Tsulaia¹⁸, S. Tsuno⁸¹, O. Tsur¹⁵⁹, D. Tsybychev¹⁵⁴, Y. Tu^{62b},
A. Tudorache^{27b}, V. Tudorache^{27b}, A.N. Tuna³⁶, S. Turchikhin⁷⁹, D. Turgeman¹⁷⁸, I. Turk Cakir^{4b,u},
R.J. Turner²¹, R. Turra^{68a}, P.M. Tuts³⁹, S. Tzamarias¹⁶¹, P. Tzanis¹⁰, E. Tzovara⁹⁹, K. Uchida¹⁶²,
F. Ukegawa¹⁶⁷, G. Unal³⁶, M. Unal¹¹, A. Undrus²⁹, G. Unel¹⁶⁹, F.C. Ungaro¹⁰⁴, K. Uno¹⁶², J. Urban^{28b},
P. Urquijo¹⁰⁴, G. Usai⁸, R. Ushioda¹⁶³, Z. Uysal^{12d}, V. Vacek¹⁴⁰, B. Vachon¹⁰³, K.O.H. Vadla¹³²,
T. Vafeiadis³⁶, C. Valderanis¹¹³, E. Valdes Santurio^{45a,45b}, M. Valente^{166a}, S. Valentinetti^{23b,23a},
A. Valero¹⁷², L. Val ry⁴⁶, R.A. Vallance²¹, A. Vallier³⁶, J.A. Valls Ferrer¹⁷², T.R. Van Daalen¹⁴,
P. Van Gemmeren⁶, S. Van Stroud⁹⁴, I. Van Vulpen¹¹⁹, M. Vanadia^{73a,73b}, W. Vandelli³⁶,
M. Vandenbroucke¹⁴³, E.R. Vandewall¹²⁸, D. Vannicola^{72a,72b}, L. Vannoli^{55b,55a}, R. Vari^{72a},
E.W. Varnes⁷, C. Varni^{55b,55a}, T. Varol¹⁵⁷, D. Varouchas⁶⁴, K.E. Varvell¹⁵⁶, M.E. Vasile^{27b}, L. Vaslin³⁸,
G.A. Vasquez¹⁷⁴, F. Vazeille³⁸, D. Vazquez Furelos¹⁴, T. Vazquez Schroeder³⁶, J. Veatch⁵³, V. Vecchio¹⁰⁰,
M.J. Veen¹¹⁹, L.M. Veloce¹⁶⁵, F. Veloso^{138a,138c}, S. Veneziano^{72a}, A. Ventura^{67a,67b}, A. Verbytskyi¹¹⁴,
M. Verducci^{71a,71b}, C. Vergis²⁴, M. Verissimo De Araujo^{80b}, W. Verkerke¹¹⁹, A.T. Vermeulen¹¹⁹,
J.C. Vermeulen¹¹⁹, C. Vernieri¹⁵², P.J. Verschuuren⁹³, M.L. Vesterbacka¹²⁴, M.C. Vetterli^{151,ak},
N. Viaux Maira^{145d}, T. Vickey¹⁴⁸, O.E. Vickey Boeriu¹⁴⁸, G.H.A. Viehhauser¹³³, L. Vigani^{61b},
M. Villa^{23b,23a}, M. Villaplana Perez¹⁷², E.M. Villhauer⁵⁰, E. Vilucchi⁵¹, M.G. Vincter³⁴, G.S. Virdee²¹,
A. Vishwakarma⁵⁰, C. Vittori^{23b,23a}, I. Vivarelli¹⁵⁵, V. Vladimirov¹⁷⁶, M. Vogel¹⁸⁰, P. Vokac¹⁴⁰,
J. Von Ahnen⁴⁶, S.E. von Buddenbrock^{33f}, E. Von Toerne²⁴, V. Vorobel¹⁴¹, K. Vorobev¹¹¹, M. Vos¹⁷²,
J.H. Vossebeld⁹⁰, M. Vozak¹⁰⁰, N. Vranjes¹⁶, M. Vranjes Milosavljevic¹⁶, V. Vrba^{140,*}, M. Vreeswijk¹¹⁹,
N.K. Vu¹⁰¹, R. Vuillermet³⁶, I. Vukotic³⁷, S. Wada¹⁶⁷, C. Wagner¹⁰², P. Wagner²⁴, W. Wagner¹⁸⁰,
S. Wahdan¹⁸⁰, H. Wahlberg⁸⁸, R. Wakasa¹⁶⁷, M. Wakida¹¹⁶, V.M. Walbrecht¹¹⁴, J. Walder¹⁴²,
R. Walker¹¹³, S.D. Walker⁹³, W. Walkowiak¹⁵⁰, V. Wallangen^{45a,45b}, A.M. Wang⁵⁹, A.Z. Wang¹⁷⁹,
C. Wang^{60a}, C. Wang^{60c}, H. Wang¹⁸, J. Wang^{62a}, P. Wang⁴², R.-J. Wang⁹⁹, R. Wang⁵⁹, R. Wang¹²⁰,
S.M. Wang¹⁵⁷, S. Wang^{60b}, T. Wang^{60a}, W.T. Wang^{60a}, W.X. Wang^{60a}, X. Wang¹⁷¹, Y. Wang^{60a},
Z. Wang¹⁰⁵, C. Wanotayaroj³⁶, A. Warburton¹⁰³, C.P. Ward³², R.J. Ward²¹, N. Warrack⁵⁷, A.T. Watson²¹,
M.F. Watson²¹, G. Watts¹⁴⁷, B.M. Waugh⁹⁴, A.F. Webb¹¹, C. Weber²⁹, M.S. Weber²⁰, S.A. Weber³⁴,
S.M. Weber^{61a}, C. Wei^{60a}, Y. Wei¹³³, A.R. Weidberg¹³³, J. Weingarten⁴⁷, M. Weirich⁹⁹, C. Weiser⁵²,
P.S. Wells³⁶, T. Wenaus²⁹, B. Wendland⁴⁷, T. Wengler³⁶, S. Wenig³⁶, N. Vermes²⁴, M. Wessels^{61a},
T.D. Weston²⁰, K. Whalen¹³⁰, A.M. Wharton⁸⁹, A.S. White⁵⁹, A. White⁸, M.J. White¹, D. Whiteson¹⁶⁹,
W. Wiedenmann¹⁷⁹, C. Wiel⁴⁸, M. Wielers¹⁴², N. Wieseotte⁹⁹, C. Wiglesworth⁴⁰, L.A.M. Wiik-Fuchs⁵²,
H.G. Wilkens³⁶, L.J. Wilkins⁹³, D.M. Williams³⁹, H.H. Williams¹³⁵, S. Williams³², S. Willocq¹⁰²,
P.J. Windischhofer¹³³, I. Wingerter-Seez⁵, F. Winklmeier¹³⁰, B.T. Winter⁵², M. Wittgen¹⁵²,
M. Wobisch⁹⁵, A. Wolf⁹⁹, R. W lker¹³³, J. Wollrath⁵², M.W. Wolter⁸⁴, H. Wolters^{138a,138c},
V.W.S. Wong¹⁷³, A.F. Wongel⁴⁶, N.L. Woods¹⁴⁴, S.D. Worm⁴⁶, B.K. Wosiek⁸⁴, K.W. Woźniak⁸⁴,
K. Wraight⁵⁷, J. Wu^{15a,15d}, S.L. Wu¹⁷⁹, X. Wu⁵⁴, Y. Wu^{60a}, Z. Wu¹⁴³, J. Wuerzinger¹³³, T.R. Wyatt¹⁰⁰,
B.M. Wynne⁵⁰, S. Xella⁴⁰, J. Xiang^{62c}, X. Xiao¹⁰⁵, X. Xie^{60a}, I. Xioidis¹⁵⁵, D. Xu^{15a}, H. Xu^{60a}, H. Xu^{60a},
L. Xu^{60a}, R. Xu¹³⁵, W. Xu¹⁰⁵, Y. Xu^{15b}, Z. Xu^{60b}, Z. Xu¹⁵², B. Yabsley¹⁵⁶, S. Yacoob^{33a}, D.P. Yallup⁹⁴,
N. Yamaguchi⁸⁷, Y. Yamaguchi¹⁶³, M. Yamatani¹⁶², H. Yamauchi¹⁶⁷, T. Yamazaki¹⁸, Y. Yamazaki⁸²,

J. Yan^{60c}, Z. Yan²⁵, H.J. Yang^{60c,60d}, H.T. Yang¹⁸, S. Yang^{60a}, T. Yang^{62c}, X. Yang^{60a}, X. Yang^{15a},
 Y. Yang¹⁶², Z. Yang^{105,60a}, W.-M. Yao¹⁸, Y.C. Yap⁴⁶, H. Ye^{15c}, J. Ye⁴², S. Ye²⁹, I. Yeletsikh⁷⁹,
 M.R. Yexley⁸⁹, P. Yin³⁹, K. Yorita¹⁷⁷, K. Yoshihara⁷⁸, C.J.S. Young³⁶, C. Young¹⁵², R. Yuan^{60b,j}, X. Yue^{61a},
 M. Zaazoua^{35f}, B. Zabinski⁸⁴, G. Zacharis¹⁰, E. Zaffaroni⁵⁴, J. Zahreddine¹⁰¹, A.M. Zaitsev^{122,af},
 T. Zakareishvili^{158b}, N. Zakharchuk³⁴, S. Zambito³⁶, D. Zanzi⁵², S.V. Zeiřner⁴⁷, C. Zeitnitz¹⁸⁰,
 G. Zemaityte¹³³, J.C. Zeng¹⁷¹, O. Zenin¹²², T. Ženiř^{28a}, S. Zenz⁹², S. Zerradi^{35a}, D. Zerwas⁶⁴,
 M. Zgubič¹³³, B. Zhang^{15c}, D.F. Zhang^{15b}, G. Zhang^{15b}, J. Zhang⁶, K. Zhang^{15a}, L. Zhang^{15c},
 M. Zhang¹⁷¹, R. Zhang¹⁷⁹, S. Zhang¹⁰⁵, X. Zhang^{60c}, X. Zhang^{60b}, Z. Zhang⁶⁴, P. Zhao⁴⁹, Y. Zhao¹⁴⁴,
 Z. Zhao^{60a}, A. Zhemchugov⁷⁹, Z. Zheng¹⁰⁵, D. Zhong¹⁷¹, B. Zhou¹⁰⁵, C. Zhou¹⁷⁹, H. Zhou⁷, M. Zhou¹⁵⁴,
 N. Zhou^{60c}, Y. Zhou⁷, C.G. Zhu^{60b}, C. Zhu^{15a,15d}, H.L. Zhu^{60a}, H. Zhu^{15a}, J. Zhu¹⁰⁵, Y. Zhu^{60a},
 X. Zhuang^{15a}, K. Zhukov¹¹⁰, V. Zhulanov^{121b,121a}, D. Zieminska⁶⁵, N.I. Zimine⁷⁹, S. Zimmermann^{52,*},
 Z. Zinonos¹¹⁴, M. Ziolkowski¹⁵⁰, L. Živković¹⁶, A. Zoccoli^{23b,23a}, K. Zoch⁵³, T.G. Zorbas¹⁴⁸, R. Zou³⁷,
 W. Zou³⁹, L. Zwalinski³⁶

¹ Department of Physics, University of Adelaide, Adelaide, Australia

² Physics Department, SUNY Albany, Albany NY, United States of America

³ Department of Physics, University of Alberta, Edmonton AB, Canada

⁴ (a) Department of Physics, Ankara University, Ankara; (b) Istanbul Aydın University, Application and Research Center for Advanced Studies, Istanbul; (c) Division of Physics, TOBB University of Economics and Technology, Ankara, Turkey

⁵ LAPP, Univ. Savoie Mont Blanc, CNRS/IN2P3, Annecy, France

⁶ High Energy Physics Division, Argonne National Laboratory, Argonne IL, United States of America

⁷ Department of Physics, University of Arizona, Tucson AZ, United States of America

⁸ Department of Physics, University of Texas at Arlington, Arlington TX, United States of America

⁹ Physics Department, National and Kapodistrian University of Athens, Athens, Greece

¹⁰ Physics Department, National Technical University of Athens, Zografou, Greece

¹¹ Department of Physics, University of Texas at Austin, Austin TX, United States of America

¹² (a) Bahcesehir University, Faculty of Engineering and Natural Sciences, Istanbul; (b) Istanbul Bilgi University, Faculty of Engineering and Natural Sciences, Istanbul; (c) Department of Physics, Bogazici University, Istanbul; (d) Department of Physics Engineering, Gaziantep University, Gaziantep, Turkey

¹³ Institute of Physics, Azerbaijan Academy of Sciences, Baku, Azerbaijan

¹⁴ Institut de Física d'Altes Energies (IFAE), Barcelona Institute of Science and Technology, Barcelona, Spain

¹⁵ (a) Institute of High Energy Physics, Chinese Academy of Sciences, Beijing; (b) Physics Department, Tsinghua University, Beijing; (c) Department of Physics, Nanjing University, Nanjing;

(d) University of Chinese Academy of Science (UCAS), Beijing, China

¹⁶ Institute of Physics, University of Belgrade, Belgrade, Serbia

¹⁷ Department for Physics and Technology, University of Bergen, Bergen, Norway

¹⁸ Physics Division, Lawrence Berkeley National Laboratory and University of California, Berkeley CA, United States of America

¹⁹ Institut für Physik, Humboldt Universität zu Berlin, Berlin, Germany

²⁰ Albert Einstein Center for Fundamental Physics and Laboratory for High Energy Physics, University of Bern, Bern, Switzerland

²¹ School of Physics and Astronomy, University of Birmingham, Birmingham, United Kingdom

²² (a) Facultad de Ciencias y Centro de Investigaciones, Universidad Antonio Nariño, Bogotá; (b) Departamento de Física, Universidad Nacional de Colombia, Bogotá, Colombia, Colombia

²³ (a) INFN Bologna and Università di Bologna, Dipartimento di Fisica; (b) INFN Sezione di Bologna, Italy

²⁴ Physikalisches Institut, Universität Bonn, Bonn, Germany

²⁵ Department of Physics, Boston University, Boston MA, United States of America

²⁶ Department of Physics, Brandeis University, Waltham MA, United States of America

²⁷ (a) Transilvania University of Brasov, Brasov; (b) Horia Hulubei National Institute of Physics and Nuclear Engineering, Bucharest; (c) Department of Physics, Alexandru Ioan Cuza University of Iasi, Iasi; (d) National Institute for Research and Development of Isotopic and Molecular Technologies, Physics Department, Cluj-Napoca; (e) University Politehnica Bucharest, Bucharest; (f) West University in Timisoara, Timisoara, Romania

²⁸ (a) Faculty of Mathematics, Physics and Informatics, Comenius University, Bratislava; (b) Department of Subnuclear Physics, Institute of Experimental Physics of the Slovak Academy of Sciences, Kosice, Slovak Republic

²⁹ Physics Department, Brookhaven National Laboratory, Upton NY, United States of America

³⁰ Departamento de Física, Universidad de Buenos Aires, Buenos Aires, Argentina

³¹ California State University, CA, United States of America

³² Cavendish Laboratory, University of Cambridge, Cambridge, United Kingdom

³³ (a) Department of Physics, University of Cape Town, Cape Town; (b) iThema Labs, Western Cape; (c) Department of Mechanical Engineering Science, University of Johannesburg, Johannesburg; (d) National Institute of Physics, University of the Philippines Diliman; (e) University of South Africa, Department of Physics, Pretoria; (f) School of Physics, University of the Witwatersrand, Johannesburg, South Africa

³⁴ Department of Physics, Carleton University, Ottawa ON, Canada

³⁵ (a) Faculté des Sciences Ain Chock, Réseau Universitaire de Physique des Hautes Energies – Université Hassan II, Casablanca; (b) Faculté des Sciences, Université Ibn-Tofail, Kénitra;

(c) Faculté des Sciences Semlalia, Université Cadi Ayyad, LPHEA, Marrakech; (d) Moroccan Foundation for Advanced Science Innovation and Research (MASCIIR), Rabat; (e) LPMR, Faculté des Sciences, Université Mohamed Premier, Oujda; (f) Faculté des sciences, Université Mohammed V, Rabat, Morocco

³⁶ CERN, Geneva, Switzerland

³⁷ Enrico Fermi Institute, University of Chicago, Chicago IL, United States of America

³⁸ LPC, Université Clermont Auvergne, CNRS/IN2P3, Clermont-Ferrand, France

³⁹ Nevis Laboratory, Columbia University, Irvington NY, United States of America

⁴⁰ Niels Bohr Institute, University of Copenhagen, Copenhagen, Denmark

⁴¹ (a) Dipartimento di Fisica, Università della Calabria, Rende; (b) INFN Gruppo Collegato di Cosenza, Laboratori Nazionali di Frascati, Italy

⁴² Physics Department, Southern Methodist University, Dallas TX, United States of America

⁴³ Physics Department, University of Texas at Dallas, Richardson TX, United States of America

⁴⁴ National Centre for Scientific Research "Demokritos", Agia Paraskevi, Greece

⁴⁵ (a) Department of Physics, Stockholm University; (b) Oskar Klein Centre, Stockholm, Sweden

⁴⁶ Deutsches Elektronen-Synchrotron DESY, Hamburg and Zeuthen, Germany

⁴⁷ Lehrstuhl für Experimentelle Physik IV, Technische Universität Dortmund, Dortmund, Germany

⁴⁸ Institut für Kern- und Teilchenphysik, Technische Universität Dresden, Dresden, Germany

⁴⁹ Department of Physics, Duke University, Durham NC, United States of America

⁵⁰ SUPA – School of Physics and Astronomy, University of Edinburgh, Edinburgh, United Kingdom

- 51 INFN e Laboratori Nazionali di Frascati, Frascati, Italy
- 52 Physikalisches Institut, Albert-Ludwigs-Universität Freiburg, Freiburg, Germany
- 53 II. Physikalisches Institut, Georg-August-Universität Göttingen, Göttingen, Germany
- 54 Département de Physique Nucléaire et Corpusculaire, Université de Genève, Genève, Switzerland
- 55 (a) Dipartimento di Fisica, Università di Genova, Genova; (b) INFN Sezione di Genova, Italy
- 56 II. Physikalisches Institut, Justus-Liebig-Universität Giessen, Giessen, Germany
- 57 SUPA – School of Physics and Astronomy, University of Glasgow, Glasgow, United Kingdom
- 58 LPSC, Université Grenoble Alpes, CNRS/IN2P3, Grenoble INP, Grenoble, France
- 59 Laboratory for Particle Physics and Cosmology, Harvard University, Cambridge MA, United States of America
- 60 (a) Department of Modern Physics and State Key Laboratory of Particle Detection and Electronics, University of Science and Technology of China, Hefei; (b) Institute of Frontier and Interdisciplinary Science and Key Laboratory of Particle Physics and Particle Irradiation (MOE), Shandong University, Qingdao; (c) School of Physics and Astronomy, Shanghai Jiao Tong University, Key Laboratory for Particle Astrophysics and Cosmology (MOE), SKLPPC, Shanghai; (d) Tsung-Dao Lee Institute, Shanghai, China
- 61 (a) Kirchhoff-Institut für Physik, Ruprecht-Karls-Universität Heidelberg, Heidelberg; (b) Physikalisches Institut, Ruprecht-Karls-Universität Heidelberg, Heidelberg, Germany
- 62 (a) Department of Physics, Chinese University of Hong Kong, Shatin, N.T., Hong Kong; (b) Department of Physics, University of Hong Kong, Hong Kong; (c) Department of Physics and Institute for Advanced Study, Hong Kong University of Science and Technology, Clear Water Bay, Kowloon, Hong Kong, China
- 63 Department of Physics, National Tsing Hua University, Hsinchu, Taiwan
- 64 IJCLab, Université Paris-Saclay, CNRS/IN2P3, 91405, Orsay, France
- 65 Department of Physics, Indiana University, Bloomington IN, United States of America
- 66 (a) INFN Gruppo Collegato di Udine, Sezione di Trieste, Udine; (b) ICTP, Trieste; (c) Dipartimento Politecnico di Ingegneria e Architettura, Università di Udine, Udine, Italy
- 67 (a) INFN Sezione di Lecce; (b) Dipartimento di Matematica e Fisica, Università del Salento, Lecce, Italy
- 68 (a) INFN Sezione di Milano; (b) Dipartimento di Fisica, Università di Milano, Milano, Italy
- 69 (a) INFN Sezione di Napoli; (b) Dipartimento di Fisica, Università di Napoli, Napoli, Italy
- 70 (a) INFN Sezione di Pavia; (b) Dipartimento di Fisica, Università di Pavia, Pavia, Italy
- 71 (a) INFN Sezione di Pisa; (b) Dipartimento di Fisica E. Fermi, Università di Pisa, Pisa, Italy
- 72 (a) INFN Sezione di Roma; (b) Dipartimento di Fisica, Sapienza Università di Roma, Roma, Italy
- 73 (a) INFN Sezione di Roma Tor Vergata; (b) Dipartimento di Fisica, Università di Roma Tor Vergata, Roma, Italy
- 74 (a) INFN Sezione di Roma Tre; (b) Dipartimento di Matematica e Fisica, Università Roma Tre, Roma, Italy
- 75 (a) INFN-TIFPA; (b) Università degli Studi di Trento, Trento, Italy
- 76 Institut für Astro- und Teilchenphysik, Leopold-Franzens-Universität, Innsbruck, Austria
- 77 University of Iowa, Iowa City IA, United States of America
- 78 Department of Physics and Astronomy, Iowa State University, Ames IA, United States of America
- 79 Joint Institute for Nuclear Research, Dubna, Russia
- 80 (a) Departamento de Engenharia Elétrica, Universidade Federal de Juiz de Fora (UFJF), Juiz de Fora; (b) Universidade Federal do Rio De Janeiro COPPE/EE/IF, Rio de Janeiro; (c) Instituto de Física, Universidade de São Paulo, São Paulo, Brazil
- 81 KEK, High Energy Accelerator Research Organization, Tsukuba, Japan
- 82 Graduate School of Science, Kobe University, Kobe, Japan
- 83 (a) AGH University of Science and Technology, Faculty of Physics and Applied Computer Science, Krakow; (b) Marian Smoluchowski Institute of Physics, Jagiellonian University, Krakow, Poland
- 84 Institute of Nuclear Physics Polish Academy of Sciences, Krakow, Poland
- 85 Faculty of Science, Kyoto University, Kyoto, Japan
- 86 Kyoto University of Education, Kyoto, Japan
- 87 Research Center for Advanced Particle Physics and Department of Physics, Kyushu University, Fukuoka, Japan
- 88 Instituto de Física La Plata, Universidad Nacional de La Plata and CONICET, La Plata, Argentina
- 89 Physics Department, Lancaster University, Lancaster, United Kingdom
- 90 Oliver Lodge Laboratory, University of Liverpool, Liverpool, United Kingdom
- 91 Department of Experimental Particle Physics, Jožef Stefan Institute and Department of Physics, University of Ljubljana, Ljubljana, Slovenia
- 92 School of Physics and Astronomy, Queen Mary University of London, London, United Kingdom
- 93 Department of Physics, Royal Holloway University of London, Egham, United Kingdom
- 94 Department of Physics and Astronomy, University College London, London, United Kingdom
- 95 Louisiana Tech University, Ruston LA, United States of America
- 96 Fysiska institutionen, Lunds universitet, Lund, Sweden
- 97 Centre de Calcul de l'Institut National de Physique Nucléaire et de Physique des Particules (IN2P3), Villeurbanne, France
- 98 Departamento de Física Teórica C-15 and CIAFF, Universidad Autónoma de Madrid, Madrid, Spain
- 99 Institut für Physik, Universität Mainz, Mainz, Germany
- 100 School of Physics and Astronomy, University of Manchester, Manchester, United Kingdom
- 101 CPPM, Aix-Marseille Université, CNRS/IN2P3, Marseille, France
- 102 Department of Physics, University of Massachusetts, Amherst MA, United States of America
- 103 Department of Physics, McGill University, Montreal QC, Canada
- 104 School of Physics, University of Melbourne, Victoria, Australia
- 105 Department of Physics, University of Michigan, Ann Arbor MI, United States of America
- 106 Department of Physics and Astronomy, Michigan State University, East Lansing MI, United States of America
- 107 B.I. Stepanov Institute of Physics, National Academy of Sciences of Belarus, Minsk, Belarus
- 108 Research Institute for Nuclear Problems of Byelorussian State University, Minsk, Belarus
- 109 Group of Particle Physics, University of Montreal, Montreal QC, Canada
- 110 P.N. Lebedev Physical Institute of the Russian Academy of Sciences, Moscow, Russia
- 111 National Research Nuclear University MEPhI, Moscow, Russia
- 112 D.V. Skobel'syn Institute of Nuclear Physics, M.V. Lomonosov Moscow State University, Moscow, Russia
- 113 Fakultät für Physik, Ludwig-Maximilians-Universität München, München, Germany
- 114 Max-Planck-Institut für Physik (Werner-Heisenberg-Institut), München, Germany
- 115 Nagasaki Institute of Applied Science, Nagasaki, Japan
- 116 Graduate School of Science and Kobayashi-Maskawa Institute, Nagoya University, Nagoya, Japan
- 117 Department of Physics and Astronomy, University of New Mexico, Albuquerque NM, United States of America
- 118 Institute for Mathematics, Astrophysics and Particle Physics, Radboud University/Nikhef, Nijmegen, Netherlands
- 119 Nikhef National Institute for Subatomic Physics and University of Amsterdam, Amsterdam, Netherlands
- 120 Department of Physics, Northern Illinois University, DeKalb IL, United States of America
- 121 (a) Budker Institute of Nuclear Physics and NSU, SB RAS, Novosibirsk; (b) Novosibirsk State University Novosibirsk, Russia
- 122 Institute for High Energy Physics of the National Research Centre Kurchatov Institute, Protvino, Russia
- 123 Institute for Theoretical and Experimental Physics named by A.I. Alikhanov of National Research Centre "Kurchatov Institute", Moscow, Russia
- 124 Department of Physics, New York University, New York NY, United States of America
- 125 Ochanomizu University, Otsuka, Bunkyo-ku, Tokyo, Japan

- 126 Ohio State University, Columbus OH, United States of America
 127 Homer L. Dodge Department of Physics and Astronomy, University of Oklahoma, Norman OK, United States of America
 128 Department of Physics, Oklahoma State University, Stillwater OK, United States of America
 129 Palacký University, RCPTM, Joint Laboratory of Optics, Olomouc, Czech Republic
 130 Institute for Fundamental Science, University of Oregon, Eugene, OR, United States of America
 131 Graduate School of Science, Osaka University, Osaka, Japan
 132 Department of Physics, University of Oslo, Oslo, Norway
 133 Department of Physics, Oxford University, Oxford, United Kingdom
 134 LPNHE, Sorbonne Université, Université de Paris, CNRS/IN2P3, Paris, France
 135 Department of Physics, University of Pennsylvania, Philadelphia PA, United States of America
 136 Konstantinov Nuclear Physics Institute of National Research Centre “Kurchatov Institute”, PNPI, St. Petersburg, Russia
 137 Department of Physics and Astronomy, University of Pittsburgh, Pittsburgh PA, United States of America
 138 ^(a) Laboratório de Instrumentação e Física Experimental de Partículas – LIP, Lisboa; ^(b) Departamento de Física, Faculdade de Ciências, Universidade de Lisboa, Lisboa; ^(c) Departamento de Física, Universidade de Coimbra, Coimbra; ^(d) Centro de Física Nuclear da Universidade de Lisboa, Lisboa; ^(e) Departamento de Física, Universidade do Minho, Braga; ^(f) Departamento de Física Teórica y del Cosmos, Universidad de Granada, Granada (Spain); ^(g) Dep Física and CEFITEC of Faculdade de Ciências e Tecnologia, Universidade Nova de Lisboa, Caparica; ^(h) Instituto Superior Técnico, Universidade de Lisboa, Lisboa, Portugal
 139 Institute of Physics of the Czech Academy of Sciences, Prague, Czech Republic
 140 Czech Technical University in Prague, Prague, Czech Republic
 141 Charles University, Faculty of Mathematics and Physics, Prague, Czech Republic
 142 Particle Physics Department, Rutherford Appleton Laboratory, Didcot, United Kingdom
 143 IRFU, CEA, Université Paris-Saclay, Gif-sur-Yvette, France
 144 Santa Cruz Institute for Particle Physics, University of California Santa Cruz, Santa Cruz CA, United States of America
 145 ^(a) Departamento de Física, Pontificia Universidad Católica de Chile, Santiago; ^(b) Universidad Andres Bello, Department of Physics, Santiago; ^(c) Instituto de Alta Investigación, Universidad de Tarapacá; ^(d) Departamento de Física, Universidad Técnica Federico Santa María, Valparaíso, Chile
 146 Universidade Federal de São João del Rei (UFSJ), São João del Rei, Brazil
 147 Department of Physics, University of Washington, Seattle WA, United States of America
 148 Department of Physics and Astronomy, University of Sheffield, Sheffield, United Kingdom
 149 Department of Physics, Shinshu University, Nagano, Japan
 150 Department Physik, Universität Siegen, Siegen, Germany
 151 Department of Physics, Simon Fraser University, Burnaby BC, Canada
 152 SLAC National Accelerator Laboratory, Stanford CA, United States of America
 153 Physics Department, Royal Institute of Technology, Stockholm, Sweden
 154 Departments of Physics and Astronomy, Stony Brook University, Stony Brook NY, United States of America
 155 Department of Physics and Astronomy, University of Sussex, Brighton, United Kingdom
 156 School of Physics, University of Sydney, Sydney, Australia
 157 Institute of Physics, Academia Sinica, Taipei, Taiwan
 158 ^(a) E. Andronikashvili Institute of Physics, Iv. Javakishvili Tbilisi State University, Tbilisi; ^(b) High Energy Physics Institute, Tbilisi State University, Tbilisi, Georgia
 159 Department of Physics, Technion, Israel Institute of Technology, Haifa, Israel
 160 Raymond and Beverly Sackler School of Physics and Astronomy, Tel Aviv University, Tel Aviv, Israel
 161 Department of Physics, Aristotle University of Thessaloniki, Thessaloniki, Greece
 162 International Center for Elementary Particle Physics and Department of Physics, University of Tokyo, Tokyo, Japan
 163 Department of Physics, Tokyo Institute of Technology, Tokyo, Japan
 164 Tomsk State University, Tomsk, Russia
 165 Department of Physics, University of Toronto, Toronto ON, Canada
 166 ^(a) TRIUMF, Vancouver BC; ^(b) Department of Physics and Astronomy, York University, Toronto ON, Canada
 167 Division of Physics and Tomonaga Center for the History of the Universe, Faculty of Pure and Applied Sciences, University of Tsukuba, Tsukuba, Japan
 168 Department of Physics and Astronomy, Tufts University, Medford MA, United States of America
 169 Department of Physics and Astronomy, University of California Irvine, Irvine CA, United States of America
 170 Department of Physics and Astronomy, University of Uppsala, Uppsala, Sweden
 171 Department of Physics, University of Illinois, Urbana IL, United States of America
 172 Instituto de Física Corpuscular (IFIC), Centro Mixto Universidad de Valencia – CSIC, Valencia, Spain
 173 Department of Physics, University of British Columbia, Vancouver BC, Canada
 174 Department of Physics and Astronomy, University of Victoria, Victoria BC, Canada
 175 Fakultät für Physik und Astronomie, Julius-Maximilians-Universität Würzburg, Würzburg, Germany
 176 Department of Physics, University of Warwick, Coventry, United Kingdom
 177 Waseda University, Tokyo, Japan
 178 Department of Particle Physics and Astrophysics, Weizmann Institute of Science, Rehovot, Israel
 179 Department of Physics, University of Wisconsin, Madison WI, United States of America
 180 Fakultät für Mathematik und Naturwissenschaften, Fachgruppe Physik, Bergische Universität Wuppertal, Wuppertal, Germany
 181 Department of Physics, Yale University, New Haven CT, United States of America

^a Also at Borough of Manhattan Community College, City University of New York, New York NY, United States of America.

^b Also at Bruno Kessler Foundation, Trento, Italy.

^c Also at Center for High Energy Physics, Peking University, China.

^d Also at Centro Studi e Ricerche Enrico Fermi, Italy.

^e Also at CERN, Geneva, Switzerland.

^f Also at CPPM, Aix-Marseille Université, CNRS/IN2P3, Marseille, France.

^g Also at Département de Physique Nucléaire et Corpusculaire, Université de Genève, Genève, Switzerland.

^h Also at Departament de Física de la Universitat Autònoma de Barcelona, Barcelona, Spain.

ⁱ Also at Department of Financial and Management Engineering, University of the Aegean, Chios, Greece.

^j Also at Department of Physics and Astronomy, Michigan State University, East Lansing MI, United States of America.

^k Also at Department of Physics and Astronomy, University of Louisville, Louisville, KY, United States of America.

^l Also at Department of Physics, Ben Gurion University of the Negev, Beer Sheva, Israel.

^m Also at Department of Physics, California State University, East Bay, United States of America.

ⁿ Also at Department of Physics, California State University, Fresno, United States of America.

^o Also at Department of Physics, California State University, Sacramento, United States of America.

^p Also at Department of Physics, King's College London, London, United Kingdom.

^q Also at Department of Physics, St. Petersburg State Polytechnical University, St. Petersburg, Russia.

- ^r Also at Department of Physics, University of Fribourg, Fribourg, Switzerland.
- ^s Also at Faculty of Physics, M.V. Lomonosov Moscow State University, Moscow, Russia.
- ^t Also at Faculty of Physics, Sofia University, 'St. Kliment Ohridski', Sofia, Bulgaria.
- ^u Also at Giresun University, Faculty of Engineering, Giresun, Turkey.
- ^v Also at Graduate School of Science, Osaka University, Osaka, Japan.
- ^w Also at Hellenic Open University, Patras, Greece.
- ^x Also at Institucio Catalana de Recerca i Estudis Avancats, ICREA, Barcelona, Spain.
- ^y Also at Institut für Experimentalphysik, Universität Hamburg, Hamburg, Germany.
- ^z Also at Institute for Particle and Nuclear Physics, Wigner Research Centre for Physics, Budapest, Hungary.
- ^{aa} Also at Institute of Particle Physics (IPP), Canada.
- ^{ab} Also at Institute of Physics, Azerbaijan Academy of Sciences, Baku, Azerbaijan.
- ^{ac} Also at Instituto de Fisica Teorica, IFT-UAM/CSIC, Madrid, Spain.
- ^{ad} Also at Istanbul University, Dept. of Physics, Istanbul, Turkey.
- ^{ae} Also at Joint Institute for Nuclear Research, Dubna, Russia.
- ^{af} Also at Moscow Institute of Physics and Technology State University, Dolgoprudny, Russia.
- ^{ag} Also at National Research Nuclear University MEPhI, Moscow, Russia.
- ^{ah} Also at Physics Department, An-Najah National University, Nablus, Palestine.
- ^{ai} Also at Physikalisches Institut, Albert-Ludwigs-Universität Freiburg, Freiburg, Germany.
- ^{aj} Also at The City College of New York, New York NY, United States of America.
- ^{ak} Also at TRIUMF, Vancouver BC, Canada.
- ^{al} Also at Università di Napoli Parthenope, Napoli, Italy.
- ^{am} Also at University of Chinese Academy of Sciences (UCAS), Beijing, China.
- * Deceased.